FEMS Microbiology Ecology, 96, 2020, fiaa087

doi: 10.1093/femsec/fiaa087
Advance Access Publication Date: 9 May 2020
Research Article

RESEARCH ARTICLE

Global warming shifts the composition of the abundant bacterial phyllosphere microbiota as indicated by a cultivation-dependent and -independent study of the grassland phyllosphere of a long-term warming field experiment

Ebru L. Aydogan[1,†], Olga Budich[1,†], Martin Hardt[2], Young Hae Choi[3], Anne B. Jansen-Willems[4], Gerald Moser[4], Christoph Müller[4,5], Peter Kämpfer[1] and Stefanie P. Glaeser[1,*,‡]

[1]Institute of Applied Microbiology (IFZ), Justus Liebig University Giessen, D-35392 Giessen, Germany, [2]Biomedical Research Center Seltersberg – Imaging Unit, Justus Liebig University Giessen, D-35392 Giessen, Germany, [3]Natural Products Laboratory, Institute of Biology, Leiden University, Sylviusweg 72, 2333 BE Leiden, The Netherlands, [4]Institute of Plant Ecology (IFZ), Justus Liebig University Giessen, D-39392 Giessen, Germany and [5]School of Biology and Environmental Science and Earth Institute, University College Dublin, Belfield, D04V1W8 Dublin, Ireland

*Corresponding author: Institute of Applied Microbiology (IFZ), Justus Liebig University Giessen, IFZ-Heinrich-Buff-Ring 26–32, D-35392 Giessen, Germany. E-mail: Stefanie.Glaeser@umwelt.uni-giessen.de

One sentence summary: Global warming shifts the phyllosphere microbiota.

†These are shared first authors.

Editor: Angela Sessitsch

‡Stefanie P. Glaeser, http://orcid.org/0000-0001-5258-6195

ABSTRACT

The leaf-colonizing bacterial microbiota was studied in a long-term warming experiment on a permanent grassland, which had been continuously exposed to increased surface temperature (+2°C) for more than six years. Two abundant plant species, *Arrhenatherum elatius* and *Galium album*, were studied. Surface warming reduced stomata opening and changed leaf metabolite profiles. Leaf surface colonization and the concentration of leaf-associated bacterial cells were not affected. However, bacterial 16S ribosomal RNA (rRNA) gene amplicon Illumina sequencing showed significant temperature effects on the plant species-specific phyllosphere microbiota. Warming partially affected the concentrations of cultured bacteria and had a significant effect on the composition of most abundant cultured plant species-specific bacteria. The abundance of *Sphingomonas* was significantly reduced. *Sphingomonas* isolates from warmed plots represented different phylotypes, had different physiological traits and were better adapted to higher temperatures. Among *Methylobacterium* isolates, a novel phylotype with a specific *mxaF* type was cultured from plants of warmed plots while the most abundant phylotype cultured

Received: 1 November 2019; **Accepted:** 8 May 2020

from control plots was strongly reduced. This study clearly showed a correlation of long-term surface warming with changes in the plant physiology and the development of a physiologically and genetically adapted phyllosphere microbiota.

Keywords: climate change; phyllosphere; evolutionary adaptation; ecotypes; *Sphingomonas*; *Methylobacterium*

INTRODUCTION

Bacteria are the most abundant colonizers of the aerial parts of plants, the phyllosphere, with a population density of up to 10^6–10^7 bacterial cells/cm^2 leaf surface area (Lindow and Brandl 2003; Vorholt 2012). The phyllosphere is often an oligotrophic habitat, which is limited in carbon and nitrogen (Bringel and Couée 2015) and is typically inhabited by complex bacterial communities that are adapted to these conditions. The main carbon compounds present in the phyllosphere are passively leaked by plants as photoassimilates like sucrose, fructose, glucose, amino acids and organic acids (Trouvelot *et al.* 2014). Several volatile organic compounds are released by plants via stomata. Thus, the phyllosphere is an ecological niche in which bacteria are affected by annual and diurnal cycles and generally exposed to extreme variations of the environmental conditions (Vorholt 2012; Bringel and Couée 2015). Complex microbe–microbe and microbe–plant interactions drive the community compositions of phyllosphere microbes besides the plant-specific substrate availability and climatic conditions leading to a very specific ecological niche. Two abundant functionally different phyllosphere inhabitants are *Methylobacterium* spp. and *Sphingomonas* spp., both members of the *Alphaproteobacteria*. Members of the genus *Methylobacterium* are the most abundant pink-pigmented facultative methylotrophic bacteria (PPFMs) ubiquitously found in high abundances and diversity in the phyllosphere of several studied plant species (e.g. Delmotte *et al.* 2009; Wellner, Lodders and Kämpfer 2011; Knief *et al.* 2012; Bodenhausen, Horton and Bergelson 2013; Glenn, Bassett and Dowd 2015; Jo *et al.* 2015). They use methanol as main carbon source, which is released by plants as a side product of the cell wall synthesis (Delmotte *et al.* 2009). Plants benefit from PPFMs by their production of phytohormone and vitamin B12, which stimulate plant growth, health and yield (Vorholt 2012). Members of the genus *Sphingomonas* were determined as abundant phyllosphere inhabitants in several phyllosphere studies (e.g. Delmotte *et al.* 2009; Leveau and Tech 2011; Yashiro and McManus 2012; Bodenhausen, Horton and Bergelson 2013; Glenn, Bassett and Dowd 2015; Jo *et al.* 2015). The high abundance of sugar transporters of *Sphingomonas* in phyllosphere metaproteome studies indicated that carbon sugars released by plants are the main nutrients for these bacteria (Delmotte *et al.* 2009). Further studies on isolated phyllosphere *Sphingomonas* showed a high antagonistic activity against plant pathogenic bacteria (Innerebner, Knief and Vorholt 2011).

Phyllosphere-associated microbial communities are well adapted to specific plant species but can be strongly affected by changing environmental conditions that can either directly or indirectly (by affecting the plant host) induce changes of abundance, activity and community structure of the phyllosphere microbiota (Rastogi *et al.* 2012; Ren *et al.* 2014, 2015; Rico *et al.* 2014). The concentration of released methanol and the availability and composition of released carbon sugars (photoassimilates) are important plant growth-dependent factors that can indirectly influence the phyllosphere microbiota if plant growth is affected by changing environmental conditions.

Predicted from the Intergovernmental Panel on Climate Change (IPCC 2013), the global mean surface temperature will increase by 2–3°C within the next decades. The increased temperature itself and expected effects of plant growth (changes in nutrient availability for bacteria) can affect bacterial growth in the phyllosphere. In a long-term perspective, these changes may lead to shifts in the population of phyllosphere-inhabiting bacteria and the occurrence of better adapted bacteria to changed environmental conditions. Considering the 'ecotype concept' of Cohan (2002), those changing environmental conditions will drive bacterial evolution starting with the selection of adapted bacterial ecotypes and can subsequently lead to the development of novel bacterial species.

To study adaptation mechanisms of global climate change, long-term experiments are required. However, not many long-term field experiments analyzing the effect of surface warming on the phyllosphere microbiota exist (Ren *et al.* 2015; Aydogan *et al.* 2018). A first cultivation-independent study of the long-term warming experiment described here, showed that surface warming by +2°C influenced the diversity and community composition of the leaf microbiota of *Galium album*, after the grassland was exposed to elevated surface temperature for more than six years (Aydogan *et al.* 2018). However, the temperature effect on the phyllosphere microbiota in correlation with changes in plant physiology was not considered so far. Thus, we hypothesized that global climate change leads to a physiological and, in long-term perspective, evolutionary adaptation of the phyllosphere microbiota. We compared populations of phyllosphere-inhabiting bacterial taxa present at leaves of two plant species, the forb *G. album* and the grass *Arrhenatherum elatius*, grown in permanent grassland plots under control conditions and under elevated surface temperature (+2°C) after six years. Cultivation-independent and cultivation-dependent approaches, combined with the monitoring of changes in the plant physiology (stomata opening, primary leaf metabolites), focused on heterotrophic and methylotrophic bacteria representing two types of abundant nutritional specialist in the phyllosphere.

MATERIALS AND METHODS

Field site description

The experiment was performed on the permanent grassland of the Environmental Monitoring and Climate Change Impact Research Station Linden in Germany located at 50°31.6′N and 8°41.7′E at an elevation of 172 m above sea level. The site had not been ploughed for at least 100 years. During the past decades, it had been managed as a meadow with two cuts per year and fertilized with 50–80 kg N ha^{-1} year^{-1}. Since 1995, the amount of fertilizer has been reduced to 40 kg N ha^{-1} year^{-1}. The mean annual temperature and precipitation were 9.4°C and 575 mm (observation period: 1996–2005), respectively. The soil is a stagnofluvic gleysol on loamy-sandy sediments over clay (FAO classification). The vegetation is characterized as an *Arrhenatheretum elatioris* Br.Bl. *Filipendula ulmaria* subcommunity and consists of 12 grass species, 2 legumes and 15 non-leguminous herbs (Rodwell *et al.* 1992). *Arrhenatherum elatius* (monocot, grass) and *G. album* (dicot, herb) were among the most abundant plant species present in that grassland vegetation type.

Experimental setup

The surface warming experiment at a 100 m^2 site on temperate grassland was divided into 16 equally sized plots, four rows of four plots. Each plot was treated by an infrared (IR) lamp except for the control (Figure S1a, Supporting Information). An area of 318 cm^2 in the center of each plot, directly underneath the IR lamp, was used for all measurements between 2008 and 2014. The plots were randomly assigned to four different treatments. Four independent plots (one per row) were studied per treatment. Treatment plots were distributed according to a Latin square (each treatment occurred once in each row and each column; Figure S1b, Supporting Information). The treatment with a mean 2°C increase in surface temperature above ambient temperature at 5 cm above the soil surface (T1 to T4 plots) was compared to control plots of ambient temperature (C1 to C4 plots). The surface temperature on the plots was elevated using ceramic IR heaters ESE of 230 V and 250 W with reflector and E27 ceramic lamp holder (Friedr. Freek GmbH, Menden, Germany). The lamps were connected to three metal bars to provide resistance against wind damage. A metal plate above the lamps functioned as a rain protector. Different temperatures were realized by playing the IR heaters at different heights above the ground; e.g. to increase the surface temperature by 2°C (T plots), the IR heaters were placed at 80 cm above the ground. There was no IR heater but only a 'rain protector' plate above the control treatment (C plots) to ensure comparability to the other treatments. Heating commenced on 24 January 2008. Sampling was carried out after the six-year long-term experiment. Thus, the study reveals the changes after this period but cannot reveal the change during that time.

Phyllosphere sampling

Leaves of *A. elatius* (A) and *G. album* (G) were sampled on 12 May 2014 between 9 and 12 am. Samples were collected separately for both plant species from the four C and T plots, respectively. The average air temperature during sampling was 11.2°C, the precipitation rate 0.1 mm d^{-1}, the global radiation 510.9 W m^{-2} and the wind speed 6.5 km h^{-1}. Two days before sampling (10 May 2014/11 May 2014), the air temperature reached 11/11.1°C; the precipitation rate was 0.2 mm d^{-1}, the global radiation 91.2/208.4 W m^{-2} and the wind speed 2.4/5.1 km h^{-1} on average (Figure S2, Supporting Information). For *A. elatius*, the middle 4 cm of the first and second leaves were cut out by sterile scissors and pestle [always flamed with 70% (v/v) ethanol] (samples A-C1 to 4; A-T1 to 4). For *G. album*, the third wreath of leaves was collected using a sterile pestle (samples G-C1 to 4; G-T1 to 4). Leaves of three plants per species and plot were collected for total surface attached cell and microbiological analysis in two 120-mL sterile Whirl-Pak bags (Carl Roth GmbH, Karlsruhe, Germany). One bag was stored immediately at -80°C (for molecular analysis) and one stored at 4°C (cultivation, cell counting). Both were stored darkened and transported after sampling 5 km to the laboratory and either stored at -80°C or processed immediately after arriving in the laboratory (4°C samples).

Scanning electron microscopy (SEM) analysis

Leaf surface structure and bacterial colonization patterns were investigated by SEM. Four 0.5-cm-long pieces of *A. elatius* leaves and four leaves of the third wreath of leaves of *G. album* were collected for analysis. The samples were immediately fixed in 0.05 M cacodylate buffer pH 7.2, containing 1.5% formaldehyde and 1.5% glutaraldehyde at the field and subsequently transferred into fresh fixative and kept at 4°C under moderate vacuum overnight. After washing in buffer, samples were post-fixed in 1% osmium tetroxide, washed in buffer and dehydrated in an increasing ethanol series. Finally, they were critical point dried or chemically dried using hexamethyldisilazane (HMDS), mounted on SEM holders and gold sputtered.

Using the field emission SEM DSM982 (Carl Zeiss AG, Oberkochen, Germany), the number of stomata per leaf was counted from 10 electron microscopy pictures (1024 × 1024 pixels recorded at 300-fold working magnification). The size of the stomata openings (length of stomata opening) was measured from the same pictures by measuring the size of three stomata per picture. First, mean values and standard deviation for each sample (one per plot) were calculated from the 10 pictures and then mean values and standard deviations (by error propagation) were calculated over the four plots per treatment. Significant differences were tested with student's *t*-test using SigmaPlot (Applied Maths, Sint-Martens-Latem, Belgium).

Nuclear magnetic resonance (NMR) analysis of leaf metabolites

Leaf metabolites were extracted from frozen leaf material ground by using a mortar and pestle in liquid nitrogen. A modified version of the method published by Kim, Choi and Verpoorte (2010) was used. Per plot and plant species, 20 mg ground leaf material was placed in a 1.5-mL microtube and 1 mL of a mixture of 500 μL of CD_3OD and 500 μL of KH_2PO_4 buffer pH 6 in D_2O containing 0.29 mM TMSP-d_4 (trimethyl silyl propionic acid sodium salt-d_4, w/v, Sigma-Aldrich, St. Louis, MO, USA) was added. The mixture was mixed at room temperature for 1 min, and sonicated for 5 min (Branson 5510E-MT, Branson Ultrasonics, Danbury, CT, USA). After centrifugation at 17 000 × *g* at room temperature for 5 min, 300 μL of the supernatant was transferred to a 3-mm NMR glass tube and used for NMR analysis. This was performed with deuterated methanol and water, both purchased from Sigma-Aldrich . ^1H NMR spectra were recorded at 25°C on a 850 MHz Bruker AV-850 spectrometer (Bruker, Karlsruhe, Germany) operating at a proton NMR frequency of 850.13 MHz for ^1H frequency. CD_3OD was used as the internal lock. The ^1H NMR spectra were automatically reduced to ASCII files. Spectral intensities were scaled to total or internal standards (TMSP signals at δ 0.0) and reduced to integrated regions of equal width (δ 0.04) corresponding to the region of δ 0.0–10.0. The regions of δ 4.7–4.9 and δ 3.28–3.34 were excluded from the analysis because of the residual signal of D_2O and CD_3OD, respectively. Bucketing was performed by AMIX software (ver. 3.0 Bruker) with scaling on total intensity. Orthogonal projections to latent structures discriminant analysis (OPLS-DA) with Pareto scaling method was performed with the SIMCA-P+ software (v. 14.1, Umetrics, Umeå, Sweden).

Concentrations of leaf-associated bacterial cells

The concentration of leaf-attached bacterial cells (g leaf FW)$^{-1}$ was determined by SybrGreen I (SG-I) staining using the method of Lunau *et al.* (2005). Bacterial cells were detached from leaves by (i) shaking (counting of epiphytic bacteria) and (ii) mechanical treatment of leaves (counting of epi- and endophytic bacteria) in specific buffer solutions. For method (i), 1 to 2 g *A. elatius* leaves and 4 to 6 g *G. album* leaves were shaken for 10 min in sterile 50-mL falcon tubes in 30 mL autoclaved phosphate buffered saline (PBS; 130 mM NaCl, 7 mM Na_2HPO_4, 3 mM

NaH_3PO_4 per 1 liter pure water; pH 7) using a vertical shaker (level 8/Edmund Bühler, Tübingen, Germany). The detachment was repeated with further 30 mL PBS buffer. Detachment buffers were combined before further analysis. For method (ii), 0.5 g leaf material was mechanically treated in 120-mL sterile Whirl-Pak bags using 10 mL autoclaved potassium phosphate buffer (PPB; 6.75 g KH_2PO_4, 8.75 g K_2HPO_4 per 1 liter pure water) for 120 s at normal speed in a Stomacher 80 (Biomaster, Seward Laboratory Systems Inc., USA). Detached cells were fixed with 2% (v/v) glutaraldehyde (AppliChem, Darmstadt, Germany) and collected on black polycarbonate filters (0.2 μm pore size, Millipore, Eschborn, Germany) (filtered volume 0.7 mL) and stained with a SG-I (Sigma-Aldrich) Mowiol staining solution (Lunau *et al.* 2005). Stained bacterial cells on filters were visualized by epifluorescence microscopy at 1000× magnification using a Leica DFC 3000 G microscope (Leica, Wetzlar, Germany), a Leica DFC 3000 G (Leica) camera system and the LAS X software. The software was used for cell counting and cell size measurements. SG-I stained cells were counted from 10 digital images per sample. Mean values of the four plots were calculated from mean values of the 10 picture counts. The per sample standard deviations were considered by error propagation. Statistically significant differences were tested with one-way analysis of variance (ANOVA) by using the Student–Newman–Keuls (SNK) test in SigmaPlot (Applied Maths).

DNA extraction and 16S ribosomal RNA (rRNA) gene amplicon Illumina MiSeq sequencing

Bacterial community analysis by 16S rRNA gene amplicon Illumina sequencing was described in detail for *G. album* samples by Aydogan *et al.* (2018). DNA extraction of whole frozen leaves of *A. elatius* and sequence data analyses were done accordingly. But, the amplification of bacterial 16S rRNA gene sequences of *A. elatius* samples was only possible by the application of specific chloroplast and mitochondria blocking primers designed by Arenz *et al.* (2015), which were used in combination with the primer system 341F (5′-CCTACGGGNGGCWGCAG-3′) and 785R (5′-GACTACHVGGGTATCTAAKCC-3′). Thereby, the concentration of chloroplast 16S rRNA gene sequences was reduced to a relative abundance of 38.0 to 61.3% in the individual samples.

Concentration of culturable heterotrophic and methylotrophic growing bacteria

The concentration of bacteria culturable under heterotrophic ('heterotrophs') and methylotrophic ('methylotrophs') growth conditions was determined from mechanically treated leaves [method (ii), see above]. Subsamples of the buffer solutions containing detached epiphytic and partially released endophytic bacterial cells (0.5 mL) were serially diluted in autoclaved 0.2% (w/v) sodium chloride (NaCl) solution, and 100 μL of each dilution was plated in triplicates on respective growth media. Dilutions 10^0 to 10^{-4} were plated on half-concentrated R2A ($\frac{1}{2}$ R2A) agar to culture heterotrophically growing bacteria. The medium contained 1.5 g L^{-1} R2A broth (Lab M, Lancashire, UK) and 14 g agar (Roth) dissolved in pure water. Dilutions 10^0 to 10^{-3} were plated on *Methylobacterium* medium M125 (DSMZ, Braunschweig, Germany) to culture methylotrophically growing bacteria. The medium was prepared with 5 mL 0.22-μm filter-sterilized methanol as sole carbon source and 14 g three times washed agar per 1 L medium. The medium was prepared in pure water and adjusted to pH 6.8. Both media were supplemented with 200 mg L^{-1} 0.2-μm filter-sterilized cycloheximide (AppliChem) after autoclaving to avoid growth of fungi. Bacterial growth was monitored after 10 days ($\frac{1}{2}$ R2A) or 21 days (M125) of aerobic incubation at 25°C in the dark. The concentration of colony forming units (CFUs) per g leaf fresh weight (FW) was determined by counting colonies on agar plates containing between 25 and 100 colonies. Mean value and standard deviation were determined for each plot based on triplicate plating on respective media; mean values and standard deviation over the four plots, as well as tests of significant differences, were determined as described above. Most abundant and morphological different colonies were selected for phylogenetic identification. Respective bacteria were isolated by singulation streaking and stored as 20% (v/v) glycerin stocks at −80°C.

Phylogenetic identification of most abundant cultured bacteria

Cultured phyllosphere-inhabiting bacteria were identified by partial 16S rRNA gene sequencing according to Aydogan *et al.* (2016). Analyses included a first phylogenetic identification of the isolates using EzBioCloud (Yoon, Ha and Kwon 2017) and detailed phylogenetic analysis including next related type strains using ARB (Ludwig *et al.* 2004) and the 'All-Species Living Tree' project (LTP) database (Yarza *et al.* 2008) version LTPs128 (released February 2017). Isolates were assigned to phylotypes, which were defined by the formation of monophyletic clusters in the phylogenetic trees with pairwise 16S rRNA gene sequence similarities of at least 98.65–100% among the isolates present in a respective cluster. Occurrence patterns of phylotypes were used for statistical comparison in PAST3 version 3.11 (Hammer, Harper and Ryan 2001). Presence/absence of phylotypes in individual samples was used for canonical correspondence analysis (CCA) including the environmental factors—temperature and plant species.

Genotypic differentiation of *Sphingomonas* and *Methylobacterium* isolates

Detailed genotypic differentiation of *Methylobacterium* and *Sphingomonas* isolates was performed by genomic fingerprinting with two random amplified polymorphic DNA (RAPD)- polymerase chain reactions (PCRs) using primers A and B (for both, see Ziemke, Brettar and Höfle 1997) and BOX-PCR using primer BOX1AR (Versalovic *et al.* 1994). Analyses were performed according to Glaeser *et al.* (2013). Genomic fingerprint patterns generated by agarose gel electrophoresis were compared in GelCompar II version 4.5 (Applied Maths). A similarity matrix comparing the individual fingerprint patterns was calculated with the Pearson product–moment correlation (Pearson correlation). Cluster analysis was performed with the unweighted pair group method with arithmetic mean (UPGMA) with 1% position tolerance and 0.5% optimization. Isolates were assigned to one genotype if they shared identical genomic DNA fingerprint patterns.

16S–23S rRNA gene internal transcribed spacer (ITS-1) sequence analysis of *Sphingomonas* isolates

For a more detailed genotypic differentiation of *Sphingomonas* isolates, the 16S rRNA gene–23S rRNA gene internal transcribed spacer (ITS-1) sequence was analyzed. The ITS-1 sequence was amplified using the 16S rRNA gene-targeting forward

primer E786F (5′-GATTAGATACCCTGGTAG-3′) and the 23S rRNA gene-targeting reverse primer 23Sr (5′-GGGTTBCCCCATTCRG-3′) (Fisher and Triplett 1999). PCR was performed according to the amplification of the 16S rRNA gene fragments except the use of an annealing temperature of 54°C. Sanger sequencing was performed with primer 23Sr and in addition with primer 907F (5′-AAACTCAAAGGAATTGACGG-3′; Muyzer, De Waal and Uitterlinden 1993) if the whole ITS-1 could not be covered by the first reaction. Sequences were manually corrected and analyzed in MEGA5. A ribosomal rRNA operon (locus tag: Swit_R0027-Swit_R0031) of the genome sequence of *Sphingomonas wittichii* RW1^T (NC_009511) was used to determine the 3′ end of the 16S rRNA gene, the 5′ start of the 23S rRNA gene and the location of transfer RNA (tRNA) gene sequences within the ITS-1 sequence. Sequences were aligned in MEGA5 using ClustalW. Based on the sequence differences, 16S–23S ITS-1 sequence types were defined. ITS-1 sequences were divided into three fragments: the sequence from the 3′ end of the 16S rRNA gene to the isoleucine tRNA (tRNA-ILE) coding gene (ITS-1.1), the sequence between genes coding for tRNA-ILE and for the alanine tRNA (tRNA-ALA) (ITS-1.2) and the sequence after the tRNA-ALA coding gene to the 5′ start of the 23S rRNA gene (ITS-1.3). Each ITS-1 region and the tRNA coding sequences were considered separately and finally in combination to define ITS-1 based *Sphingomonas* genotypes (ITS-1 types).

MxaF nucleotide and amino acid sequence analysis of *Methylobacterium* isolates

For the differentiation of *Methylobacterium* isolates, partial sequences of the alpha subunit of the methanol dehydrogenase gene (*mxaF*) were analyzed. *MxaF* fragments were amplified with primers 1003f (5′-GCGGCACCAACTGGGGCTGGT-3′) and 1561r (5′-GGGCAGCATGAAGGGCTCCC-3′) (McDonald, Kenna and Murrell 1995) in a total volume of 25 μL as described by Wellner *et al.* (2013) except the addition of 0.2 mg mL^{-1} bovine serum albumin (BSA) to avoid the PCR inhibition by the application of cell lysates as DNA template. PCR conditions were as follows: an initial denaturation of 95°C for 3 min, 30 cycles of 95°C for 30 s, 55°C for 30 s, 72°C for 60 s and a final elongation step of 72°C for 5 min. Sanger sequencing was performed with primer 1003f. Sequence corrections and analysis were performed in MEGA5 v5.05 (Tamura *et al.* 2011) based on the chromatograms and considering the correct open reading frame (ORF) by translating the nucleotide sequence into amino acid sequences. The correct ORF was determined using the full-length *mxaF* gene sequence (locus tag: MPOP_RS22895) derived from the genome sequence of *Methylobacterium populi* BJ001^T (NC_010725.1) as reference. Partial *mxaF* nucleotide sequences were aligned according to the respective amino acid sequence-based alignment generated with ClustalW (Thompson, Higgins and Gibson 1994). Phylogenetic trees based on nucleotide and respective amino acid sequences were calculated using the neighbor-joining method and the Jukes–Cantor model (Jukes and Cantor 1969) for nucleotide sequences and the Jones-Taylor-Thornton (JTT) model (Jones, Taylor and Thornton 1992) for amino acid sequences. The analysis was based on 100 replications (bootstrap analysis) and 432 nucleotide and 141 amino acid sequence positions, respectively. Nucleotide sequences between gene sequence positions 844 and 1341 of the *mxaF* gene of *M. populi* BJ001^T were considered for allele and amino acid sequence type assignment. Each nucleotide difference or amino acid exchange was used to define a new allele (*mxaF* type) or new amino acid (MxaF type) sequence type separately and in combination of both to differentiate the *Methylobacterium* isolates based on *mxaF*/MxaF based genotype (*mxaF* type). The typing was confirmed by the clustering in respective phylogenetic trees to define isolate specific *mxaF* genotypes.

Physiological characterization of *Sphingomonas* isolates

Physiological properties of *Sphingomonas* isolates ($n = 30$) were studied using a 96-well panel test according to Kämpfer, Steiof and Dott (1991). Substrate utilization patterns, enzyme activities and acidic production were determined. For inoculation, fresh biomass of each isolate was suspended in 0.2% (w/v) autoclaved NaCl adjusted to a McFarland density of 0.5 and 50 μL of the suspension was added per well. After incubation at 25°C for 7 days, the tests were analyzed visually and photometrically using an Infinite F200PRP microplate reader and the i-control software version 2.0.10.0 (Tecan, Crailsheim, Germany). First, plate was shaken for 20 s, and then absorbance was measured by 405 nm wavelength, bandwidth of 10 nm and four flashes. Results (positive: 1; negative: 0) were used for CCA analysis in PAST3 considering temperature and plant species as environmental factors.

Growth tests of *Sphingomonas* isolates at different temperatures

Temperature-dependent growth rates were compared for *Sphingomonas* isolates ($n = 30$). One loop of fresh biomass (4 days) was used to inoculate 1 mL $\frac{1}{2}$ R2A broth in 24-well plate (Greiner Bio-One, Kremsmünster, Austria). After overnight incubation at 25°C and 100 rpm shaking in dark, the optical density (OD) was measured using an Infinite F200PRP microplate reader and the i-control software version 2.0.10.0. First, plate was shaken for 20 s, and then absorbance was measured by 595 nm wavelength, bandwidth of 10 nm, four flashes, five filled circles (3 × 3) reads per well and 1500 μm from border. The mean values of five measurements were used for calculation and adjustment to 0.05 OD with $\frac{1}{2}$ R2A broth for each isolate in triplicates in 96-well microtiter plate. Kinetic measurement for each temperature (25, 32 and 37°C) was carried out in the microplate reader for 288 cycles with 10-min interval; absorbance was measured as described above. At first, growth constant (μ) and doubling time (t_d) were calculated for each replicate using formula $\mu = (\ln X_t - \ln X_0)/(t - t_0)$, $t_d = \ln 2/\mu = 0.693/\mu$. Mean values of doubling time were used for CCA analysis in PAST3.

Sequence submissions

Nucleotide sequences generated within the project were deposit into the primary database of the International Nucleotide Sequence Database Collaboration (INSDC) under following GenBank/EMBL/DDBJ accession numbers: MN596037 to MN596160 for 16S rRNA gene sequences of identified isolates, MN610861 to MN610897 for *mxaF* sequences of *Methylobacterium* isolates and MN614059 to MN614088 for ITS-1 sequences of *Sphingomonas* isolates. Amplicon datasets of *A. elatius* samples were stored within the BioProject PRJNA578545 as BioSamples SAMN13065289 to SAMN13065296.

RESULTS

Surface warming correlated with increased stomata opening

Leaves of *G. album* and *A. elatius* grown in control (C) and elevated temperature (T) plots differed with respect to the structure of epidermal cells and stomata abundance and size. The leaf surface of *A. elatius* showed the formation of epicuticular wax crystals and contained trichomes on both leaf sides (Fig. 1A). Epicuticular wax crystals were not detected at the leaf surface of *G. album* and trichomes were only detected on the leaf edges, but not on the leaf surface (Fig. 1B). Epidermal cells of *A. elatius* were elongated, which is typical for monocots compared to short brick-shaped epidermal cells of *G. album* typical for dicots (Fig. 1A and B). *Arrhenatherum elatius* had significantly more stomata on the adaxial than the abaxial leaf side (Table S1, Supporting Information). The concentration of stomata at *G. album* leaves was, in contrast, significantly higher on the abaxial side (Figure S3, Supporting Information). Surface warming had no visible effect on the surface structure and the amount of stomata, neither on the abaxial nor on the adaxial leaf side of both plant species. However, increased surface temperature led to a significantly larger stomata opening on the abaxial leaf side of *A. elatius*; no respective effects were obtained for *G. album* (Table S2, Supporting Information).

Surface warming changed the leaf metabolomes

Different metabolite profiles were obtained for both plant species by comparative NMR score plots for leaves derived from C and T plots (Figure S4, Supporting Information). *Galium album* leaves obtained from T plots showed in comparison to leaves of C plots higher concentrations of malic acid and ethanol but a lower concentration of homoserine. *Arrhenatherum elatius* leaves derived from T plots had higher sucrose and hydroxyproline concentrations, but lower glucose concentrations. The variability of the metabolite profiles obtained for leaf samples from C plots was higher compared to that of leaves derived from T plots.

Surface warming had no effects on the colonization patterns and total abundance of phyllosphere bacteria

SEM analyses revealed that leaves of both plant species were colonized on the adaxial and abaxial leaf sides with bacterial and yeast cells of different size and shape. Difference among the species but no visible differences between C and T plots were detected (Fig. 1). Single cells and cell aggregates were mainly attached around trichomes at *A. elatius* leaves (Fig. 1C). For both plant species, bacterial cells were mainly localized next to stomata and in the cracks between epidermal leaf cells (Fig. 1C–F). Single attached and dense locally restricted surface-attached microcolonies or aggregates were obtained at the leaf surface of both plant species (Fig. 1G and H). Microcolonies and larger aggregates on the leaf surface of *A. elatius* were often formed by cells of one morphological type, mainly small rod-shaped cells (~1.1 μm in length, Fig. 1G). No visible interconnecting structures (Fig. 1G) were detected in between these aggregates. Cell aggregates determined on the surface of *G. album* leaves were larger and contained bacterial and yeast cells of different cell shapes and sizes embedded in a dense extracellular matrix (Fig. 1H). Aggregates contained also plant pollen, which were sticking in the extra polymeric matrix surrounding bacterial cells (Fig. 1H).

The concentration of leaf-associated bacteria (stained by SG-I; Figure S5, Supporting Information) was in the range of 10^6 cells (g leaf FW)$^{-1}$ for *A. elatius* and 10^5 cells (g leaf FW)$^{-1}$ for *G. album* if surface-detached cells (epiphytic bacteria) were counted (Fig. 2A), and in the range of 10^7 cells (g leaf FW)$^{-1}$ for both plant species if cells were counted after the mechanical treatment of leaves (detection of epi- and endophytic bacteria; Fig. 2B; Table S3, Supporting Information). Differences in the concentration of surface-detached cells were significant among the plant species, but warming had no significant effect. Stained bacterial cells from leaves of *A. elatius* were smaller in size compared to those obtained from *G. album* leaves. Most of the bacterial cells obtained from *A. elatius* were coccoid to coccoid-rod-shaped with a mean cell size of 0.9 (±0.7) × 0.6 (±0.3) μm. In contrast, most of the bacterial cells obtained from *G. album* leaves were rod-shaped with a mean cell size of 1.9 (±0.4) × 0.8 (±0.2) μm.

Surface warming affected the phylogenetic composition of the bacterial phyllosphere microbiota of both plant species

Bacterial 16S rRNA gene amplicon Illumina sequencing showed for both plant species significant effects of warming on the phylogenetic composition of the bacterial leaf microbiota (Fig. 3; Table 1). Non-metric multidimensional scaling (NMDS) based on Bray–Curtis distances of the bacterial community patterns resolved at the level of phylogenetic groups was used for comparative analysis. For both plant species, significant differences were obtained in the phylogenetic composition of the bacterial leaf microbiota present on plants derived from C and T plots ($P < 0.05$; Fig. 3). The bacterial community compositions of the leaf microbiota of the two different plant species were distinct but quite similar for plants derived from C plots and showed even a slight overlap for plants derived from T plots. Biplots representing environmental variables indicated that temperature as environmental variable correlated positively with significant differences between bacterial community composition and the effect of temperature was even stronger than the effect of plant species (Fig. 3).

Based on SIMPER analyses, differences of the phyllosphere microbiota composition could be associated with the temperature regime (Table 1). The three most contributing phylogenetic groups were *Sphingomonas* and *Hymenobacter* that occurred with a significant lower relative abundance in the phyllosphere microbiota of T plots, and *Pseudomonas* that occurred with a significant higher relative abundance in respective bacterial communities. Due to the high variability among the four studied plot replicates, differences were not significant for *Pseudomonas* (Table 1).

Furthermore, abundant phylogenetic groups (relative abundance > 1%), which contribute to community differences (C vs T plots), for *A. elatius* were: *Propionibacterium, Zymomonas*, *Methylobacterium*, *Aureimonas*, *Pelobacter*, uncultured *Galellales* and *Acidobacteria* subgroup 6 (occurred with a significantly lower relative abundance in T-plots), while *Nocardiodes*, uncultured *Actinobacteria* of the *Gaiellales* order, uncultured Chloroflexi (KD4–96 group) and uncultured *Spartobacteria* (DA101 soil group) occurred with a significantly higher relative abundance in T plots. Moreover, several other phylogenetic groups of minor relative abundance occurred with a significantly higher relative abundance in T plots such as several *Actinobacteria*. Abundant phylogenetic groups on *G. album* were: *Erwinia* and *Enterobacter*, which

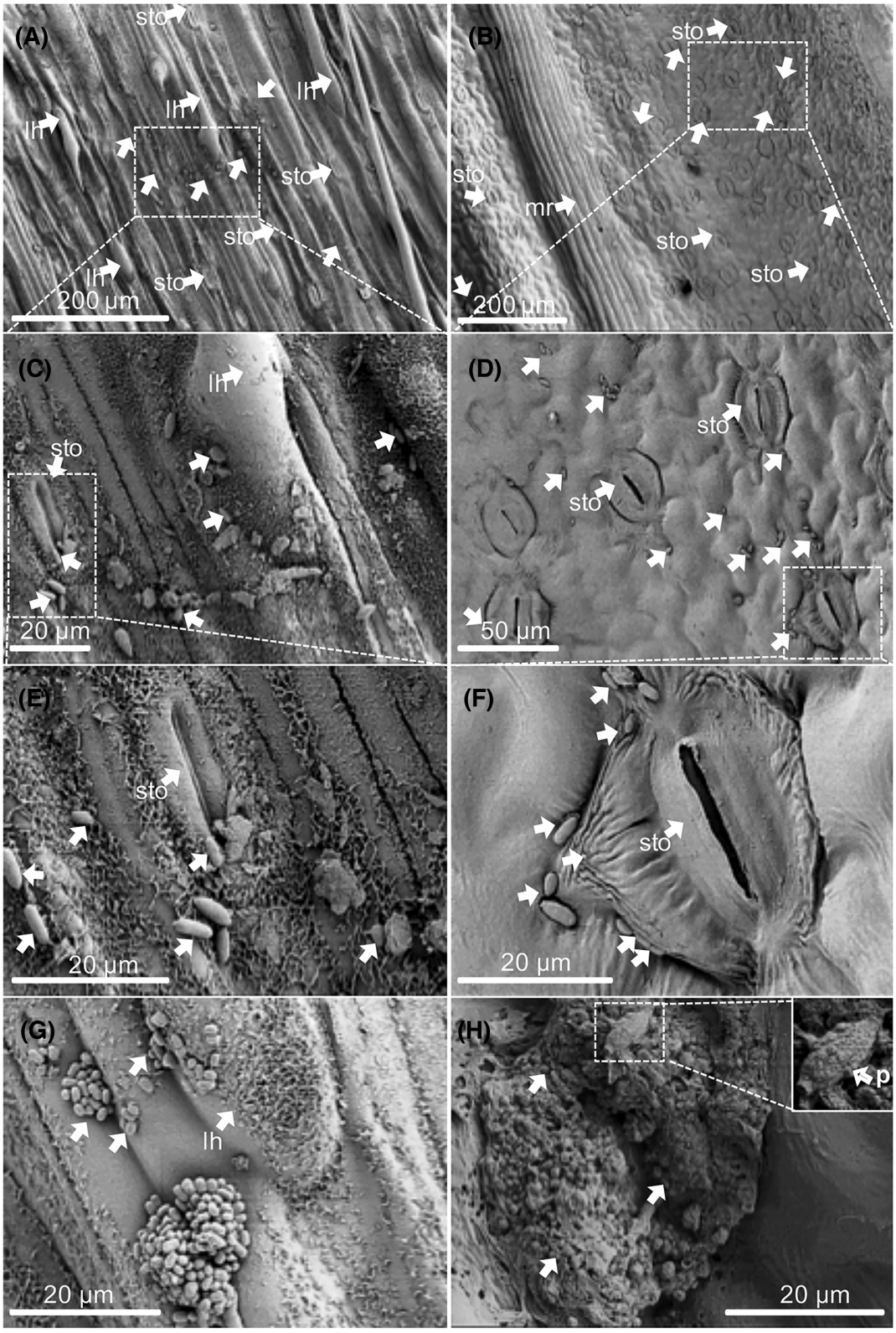

Figure 1. Colonization of the leaf surface of *A. elatius* **(A, C, E, G)** and *G. album* **(B, D, F, H)** investigated by SEM. **(A, B)** Overview of the leaf surface with stomata (sto), leaf hairs (lh), pollen (p) and bacteria (arrows). **(C)** A zoom out of **(A)** ; **(D)** a zoom out of **(B)** . Bacteria colonizing next to leaf hair **(C)** and stomata **(C, D)** and in the cracks between the plant leaf epidermal cells **(C, D)** . **(E)** A zoom out of **(C)** ; **(F)** a zoom out of **(D)** . Single bacteria at the entrance of the stomata **(E)** or next to the stomata **(E, F)** . **(H)** A zoom out of **(F)** . Microcolonies formed by a single morphological cell type **(G)** and bacterial aggregates with different cell shapes, sizes and pollen **(H)** .

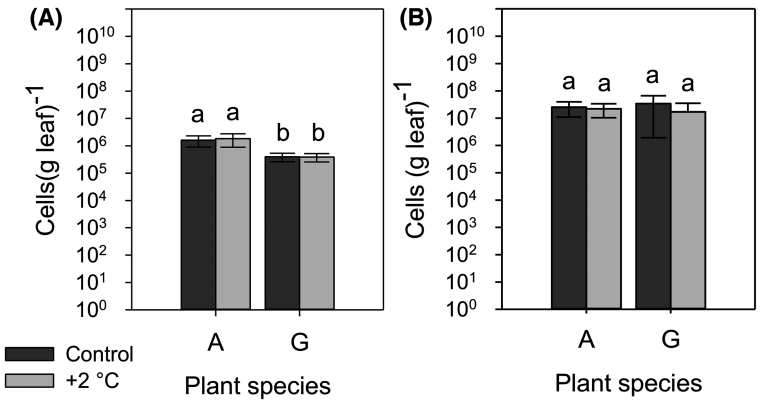

Figure 2. Concentration of total detached bacterial cells by **(A)** shaking (counting of epiphytic bacteria) and **(B)** mechanical treatment of leaves (counting of epi- and endophytic bacteria), given as cells per g leaf. Figures show differences between control plots and plots with elevated air temperature (+2°C). Mean values refer to mean values over the four plots based on 10 different cell counts for each plot. The respective standard deviation was considered by error propagation. Significance was measured with one-way ANOVA in SigmaPlot. Different letters (a, b) indicate statistical significance difference.

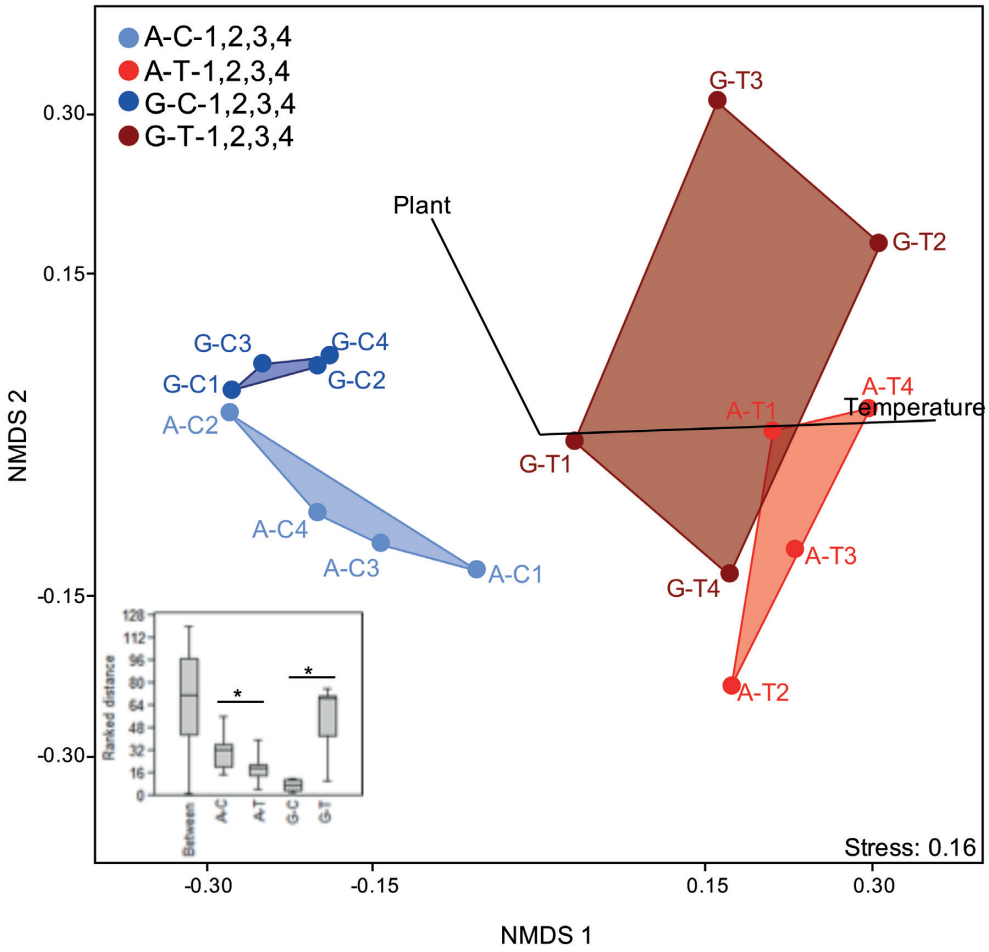

Figure 3. Impact of surface warming on the phylogenetic composition of the bacterial phyllosphere microbiota of both plant species. NMDS based on Bray–Curtis similarity matrix of the bacterial community patterns resolved at the level of phylogenetic groups illustrated for *A. elatius* (A) and *G. album* (G) leaves from plots with ambient temperature (C1 to 4) and +2°C surface temperature elevated plots (T1 to 4). Temperature and plant species were used as environmental variables represented as biplots. Rank differences of the leaf microbiota from both plant species were analyzed at the level of bacterial taxa. Box plots were calculated with the interpolated quartile method without the determination of outliers. Significant differences were determined by one-way analysis of similarities (ANOSIM). Asterisks represent statistical significance: $p < 0.05$. Analyses were performed in PAST3 version 3.11 (Hammer et al. 2001).

Table 1. Relative abundance patterns and indication of responder groups of bacterial genera present on *A. elatius* (A) and *G. album* (G) leaves grown in control (C) and warmed (T) plots. Analysis was performed at the level of phylogenetic groups (genus level). Phylogenetic groups were sorted by their contribution to the differentiation between the leaf microbiota present in plants derived from C and T plots (SIMPER analyses using PAST3). Size of the contribution is demonstrated by a colored scale. Data are shown for phylogenetic groups with ≥0.2% contribution to the total relative abundance. Individual relative abundance pattern and mean values with standard deviation among the four biological replicates per treatment are depicted. Bold values (*t*-test, $P \leq 0.05$) indicate significant differences among the relative abundance of phylogenetic groups in the phyllosphere microbiota of plants derived from C and T plots.

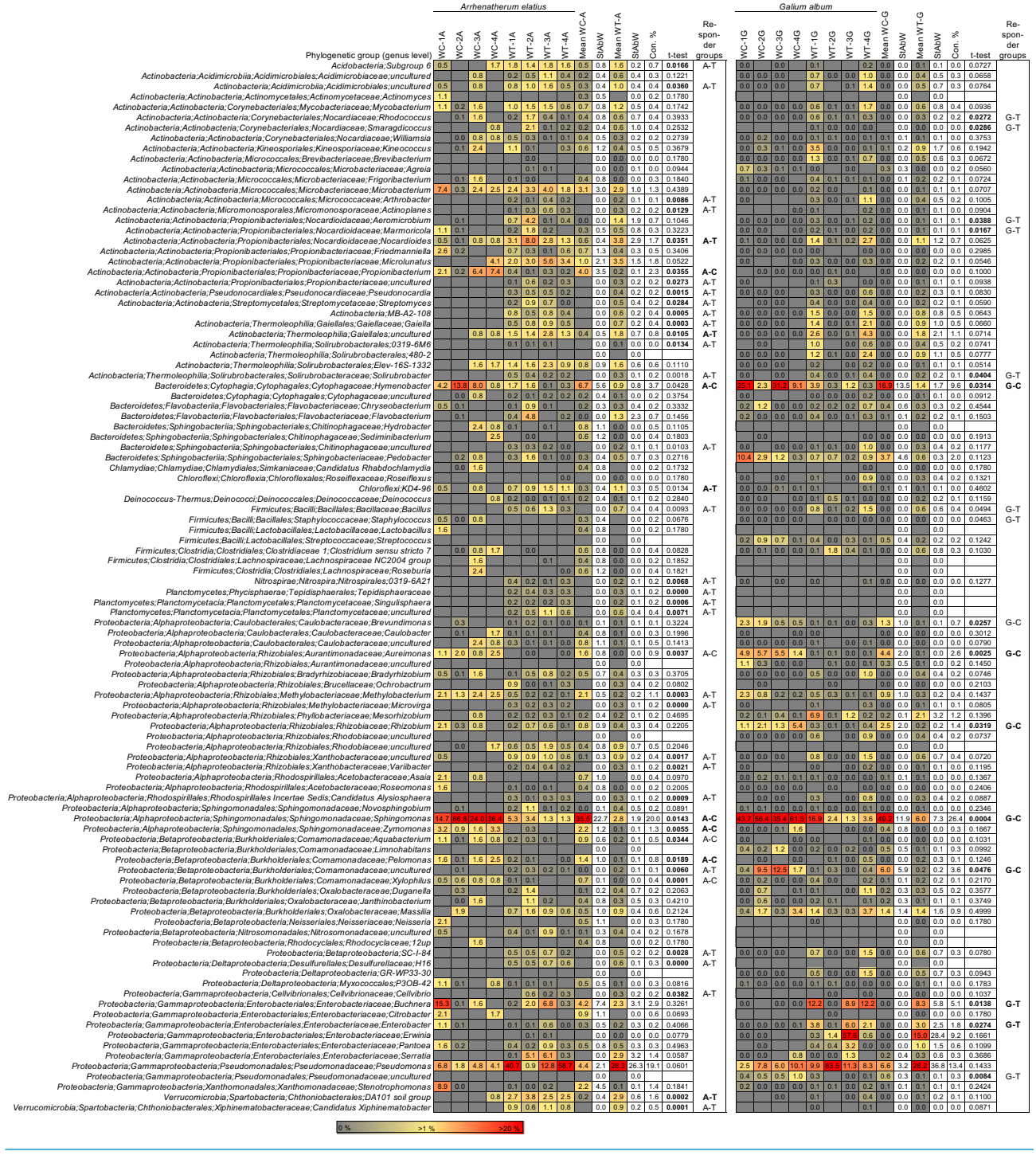

occurred with a higher relative abundance in T plots, while uncultured *Comamonadaceae*, *Aureimonas*, *Rhizobium* and *Brevundimonas* occurred with a significantly lower relative abundance in T plots. For an overview of all responder groups, see Table 1.

Concentration of culturable bacteria—plant species-specific effects of surface warming

Concentrations of heterotrophic bacteria cultured on $\frac{1}{2}$ R2A after detachment from leaves by mechanical treatment were in the same range for *A. elatius* leaves derived from C and T plots [10^6 CFUs (g leaf FW)$^{-1}$], but the concentrations obtained for *G. album* leaves from T plots [10^6 CFUs (g leaf FW)$^{-1}$] were significantly lower compared to leaves from C plots [10^7 CFUs (g leaf FW)$^{-1}$] (Fig. 4A; Table S4, Supporting Information).

The concentration of PPFM cultured under heterotrophic growth conditions was counted separately. For *A. elatius* a slightly, but not significantly, higher concentration of cultured PPFM was obtained for T compared to C plots. In contrast, for *G. album*, a slightly, but not significantly, lower concentration of PPFM was determined for leaves of T compared to C plots (Fig. 4B).

Concentrations of total bacteria cultured under methylotrophic growth conditions (methylotrophs) were in the range of 10^4–10^5 CFUs (g leaf FW)$^{-1}$ for *A. elatius* without significant differences among C and T plots (Fig. 4C). For *G. album*, the concentration of methylotrophs from leaves of T plots [4.9 ($\pm$1.8) $\times$ 10^6 CFUs (g leaf FW)$^{-1}$] was significantly lower compared to that obtained from C plots [9.7 ($\pm$3.5) $\times$ 10^6 CFUs (g leaf FW)$^{-1}$].

The separate counting of PPFM grown under methylotrophic growth condition (pink colonies only) showed no differences for *A. elatius* leaves obtained from C and T plots [10^2 CFUs (g leaf FW)$^{-1}$](Fig. 4D), but the concentration of culturable PPFMs on *G. album* leaves was significantly lower in T plots [10^4 CFUs (g leaf FW)$^{-1}$] compared to leaves obtained from C plots [10^5 CFUs (g leaf FW)$^{-1}$] (Fig. 4D).

The concentration of culturable total heterotrophs and methylotrophs was always higher for *G. album* compared to *A. elatius*. Those differences were significant for the concentrations of total cultured heterotrophic bacteria and PPFMs under control conditions. With respect to methylotrophic bacteria, significantly higher concentrations were always obtained from *G. album* leaves, while the concentrations of PPFMs cultured under heterotrophic conditions showed no significant differences between the plant species.

Surface warming selected for specific bacterial phylotypes among abundant phyllosphere colonizers

A total number of 124 of the most abundant cultured bacteria were isolated and phylogenetically identified by partial 16S rRNA gene sequencing. Isolated heterotrophic bacteria ($n = 93$) were differentiated into 56 phylotypes assigned to 28 genera of *Proteobacteria* (62%), *Actinobacteria* (30.4%) and *Bacteroidetes* (7.6%). Most of the *Proteobacteria* isolates were assigned to the genera *Sphingomonas*, *Pseudomonas*, *Methylobacterium*, *Rhizobium* and *Aureimonas*. Most of the *Actinobacteria* isolates represented *Nocardioides* spp. CCA plots based on the presence/absence of most abundant cultured heterotrophic bacterial phylotypes showed significant differences for both plant species among C and T plots (Fig. 5A) similar to differences obtained by the cultivation-independent total bacterial community analysis (Fig. 3). Temperature and plant species as environmental variables correlated with the difference of cultured bacteria as shown in CCA plots. The lower number or absence of isolates assigned to the *Sphingomonas* phylotypes S1 (C: 21, T: 2) and S11 (C: 2; T: 0) and the *Methylobacterium* phylotype M1a (C: 5, T: 0) contributed 4.2–19.0% mostly to the differences among the most abundant cultured heterotrophic bacteria of both plants grown in C compared to T plots (Table S5, Supporting Information).

Cultivation of PPFM indicated the predominance of *Methylobacterium* spp. Canonical correspondence analysis based on the diversity of most abundant PPFM (differentiated by 16S rRNA gene sequence-based phylotypes; Fig. 5B) showed a slight but not significant difference in the composition of *Methylobacterium* phylotypes on leaves of both plant species derived from C and T plots. Again, the inclusion of surface temperature as environmental variable into the CCA plots indicated a correlation of enhanced surface temperature with differences in the composition of abundant *Methylobacterium* phylotypes in C and T plots. The lower amount of phylotypes M1a (C: 15; T: 3) and M1c (C: 6; T: 3) isolated from leaves of both plant species in T compared to C plots had with 52.3 and 27.7% the strongest contribution to the differences of the *Methylobacterium* population isolated from C and T plots (Table S6, Supporting Information).

Because CCA plots showed temperature-dependent specific differences among phylotypes representing the abundant heterotrophic *Sphingomonas* spp. and methylotrophic *Methylobacterium* spp., isolates representing those two bacterial taxa were studied subsequently in more detail with respect to genetic and physiological differences among isolates obtained from C and T plot plants.

Growth of non-methylotrophic bacteria under methylotrophic growth conditions

Due to the detection of several bacterial genera not known for a methylotrophic metabolism (e.g. *Sphingomonas*, *Pseudomonas*) on agar plates with methanol as sole carbon source, growth experiments were performed with representative isolates to evaluate potential methylotrophic growth. Neither *Sphingomonas* nor *Pseudomonas* isolates were able to use methanol as sole carbon source (Figure S6, Supporting Information). Growth under methylotrophic growth conditions was thereby linked to the presence of low nutrient concentrations in the plant-derived inoculum, which led to the growth of oligotrophic bacteria. Therefore, subsequent analysis of cultured methylotrophs focused on PPFM.

Genetic diversity of cultured *Sphingomonas* with several phylo- and genotypes specifically cultured from plants derived from control and warmed plots

Sphingomonas isolates were assigned to seven phylotypes (S1, S2, S4, S6, S9, S10b, S11) differentiated based on partial 16S rRNA gene sequences (Fig. 6). Most of the *Sphingomonas* isolates (23/30 isolates) were assigned to phylotype S1 (99.4–100% intraphylotype similarity; Tables S7 and S8a, Supporting Information) clustering with *S. faeni*/*S. aurantiaca*/*S. aerolata* (99.4–99.9%). The sequence similarity between isolates of phylotype S1 and those of all other *Sphingomonas* phylotypes was low (<96.6%). Phylotypes S2 and S4, both represented by only one isolate, and phylotype S11 (2 isolates, 99.5% sequence similarity) were only obtained from leaves grown in C plots. These phylotypes were

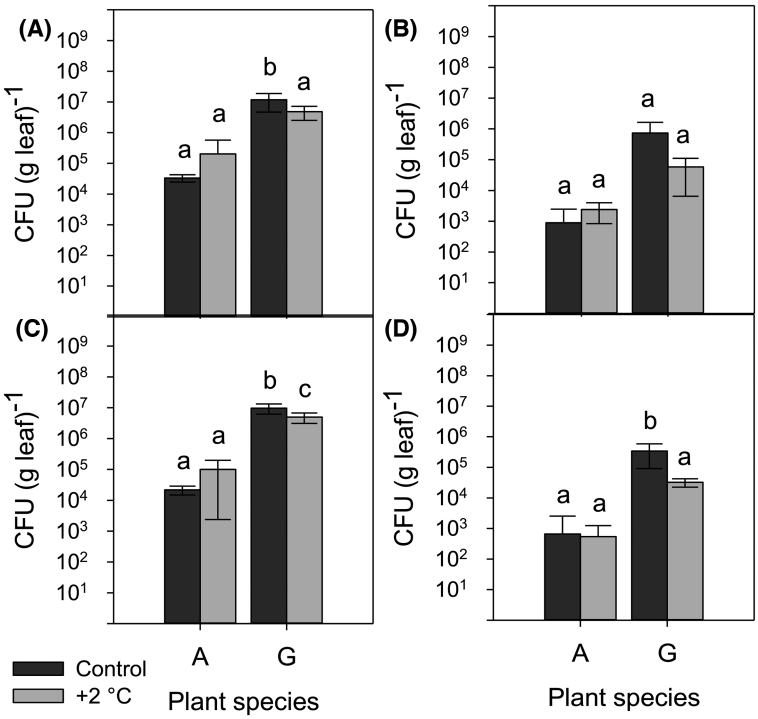

Figure 4. Concentration of culturable epiphytic and endophytic heterotrophic (**A** = total, **B** = pink pigmented) and methylotrophic (**C** = total, **D** = pink pigmented) bacteria, given as CFUs per g leaf. Figures show differences between control plots and plots with elevated air temperature (+2°C). Mean values refer to mean values over the four plots based on triplicate plating for each plot. The respective standard deviation was considered by error propagation. Significance was measured with one-way ANOVA in SigmaPlot. Different letters (a, b, c) indicate statistical significance difference.

closest related to strains of *S. melonis* (S2, 98.1%), *S. insulae* (S4, 99.6%) and *S. prati/S. arantia* (S11, 99.5–99.6%), respectively. Isolates representing phylotypes S6, S9 and S10b were all cultured from plants grown in T plots. Each phylotype was associated to type strains of different *Sphingomonas* species (S6, 98.8% *S. flavus*; S9, 97.5% *S. quilianensis*; S10b, 98.5% *S. panni*).

Sphingomonas isolates were further differentiated by genomic fingerprinting using BOX- and two RAPD-PCRs and ITS1 sequencing (Fig. 6). A total of 29 different fingerprint types and 26 different ITS1 types were determined. Considering both, isolates were assigned to 29 different genotypes. Isolates of different phylotypes represented different genotypes. In addition, nearly all isolates of phylotype S1 represented different genotypes indicating a high genetic diversity within S1. A CCA analysis based on genotype profiles for each plant species indicated that S1 genotypes were associated with different treatments. As indicated by the CCA plot, the S1 isolates derived from plants of the two plant species grown in control plots were distinct but partially similar. Interestingly, the two S1 isolates obtained from *G. album* leaves of warmed plots represented genotypes that were clearly different from those cultured from *G. album* plants grown in control plots (Fig. 6).

Sphingomonas isolates derived from T plots had specific physiological activity patterns and showed differences in temperature-dependent growth

Sphingomonas isolates ($n = 30$) were comparatively analyzed with respect to physiological traits including acidic production from carbon sources, substrate assimilation patterns, and enzyme activities and temperature-dependent growth rates at ambient and increased (37°C) temperatures. CCA plots based on the patterns of physiological traits (Fig. 7a) and temperature-dependent growth clearly showed differences for isolates derived from C and T plots. T plot isolates had distinct physiological activities (Fig. 7a) and were able to grow more efficiently under higher incubation temperatures (Fig. 7b). For physiological activity profiles of the individual isolates, see Table S9 (Supporting Information). *Sphingomonas* cultured from warmed plots had tight substrate utilization patterns, while *Sphingomonas* isolated from control plots were able to use a wider array of different carbon sources.

Warming affects the presence of specific *Methylobacterium* methylotrophic phylotypes

A total of 37 *Methylobacterium* isolates were cultured from the methylotrophic ($n = 31$) and heterotrophic ($n = 6$) growth conditions. Based on the analysis of partial 16S rRNA gene sequencing, the isolates were assigned to four different phylotypes (M1a, b, c and M3a). Most of the *Methylobacterium* isolates ($n = 18$) were assigned to phylotype M1a; those were mainly (15/18 isolates) isolated from leaves of C plots and placed within the *M. adhaesivum/M. gossipiicola/M. goesingense* cluster (Fig. 8). Isolates of phylotype M1a shared 99.3–100% partial 16S rRNA gene sequence similarity among each other and 99.1–99.2% with the type strain of *M. gossipiicola* (Tables S7 and S8b, Supporting Information). The intraphylotype similarity of the whole phylotype M1 was 97.2–100% (Table S8b, Supporting Information). Phylotype M1b was isolated once from *G. album* leaves obtained from T plots and was closest related to the type strains of *M. goesingense* (99.7%). Phylotype M1c was closely related to *M. bullatum/M. marchantiae* and isolated mainly (6/9 isolates) from leaves of C

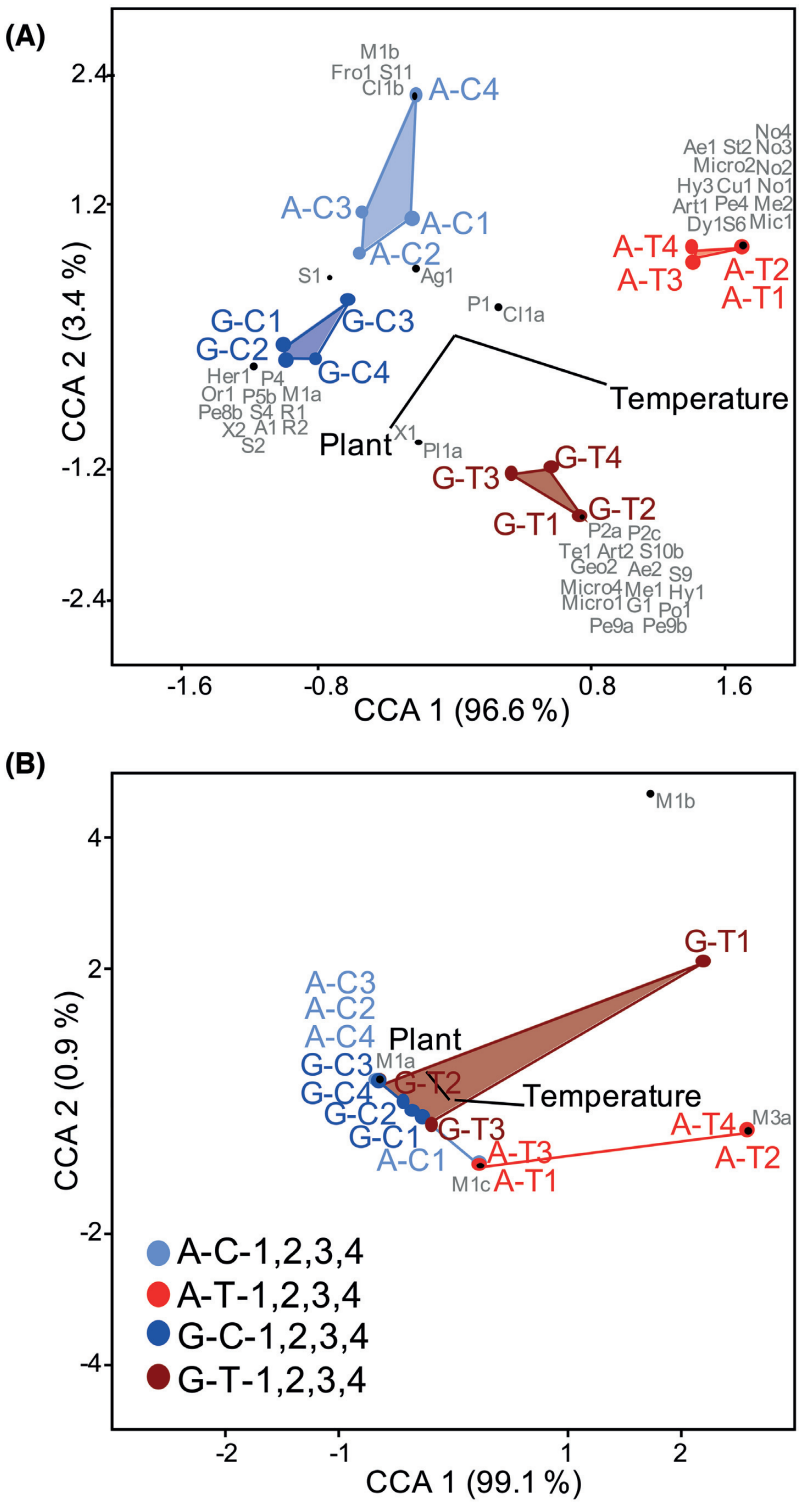

Figure 5. Impact of surface temperature on the diversity and composition of most abundant bacterial isolates cultured under heterotrophic **(A)** and methylotrophic **(B)** growth conditions. CCA of the cultured bacteria assemblages obtained from *A. elatius* (A) and *G. album* (G) leaves collected from ambient (C) and elevated surface temperature plots (T). 1,2,3,4 = biological replicates (plots). Analyses were performed in PAST3 using plant species and temperature as environmental variables. Phylotype shortcuts are explained in Fig. 4.

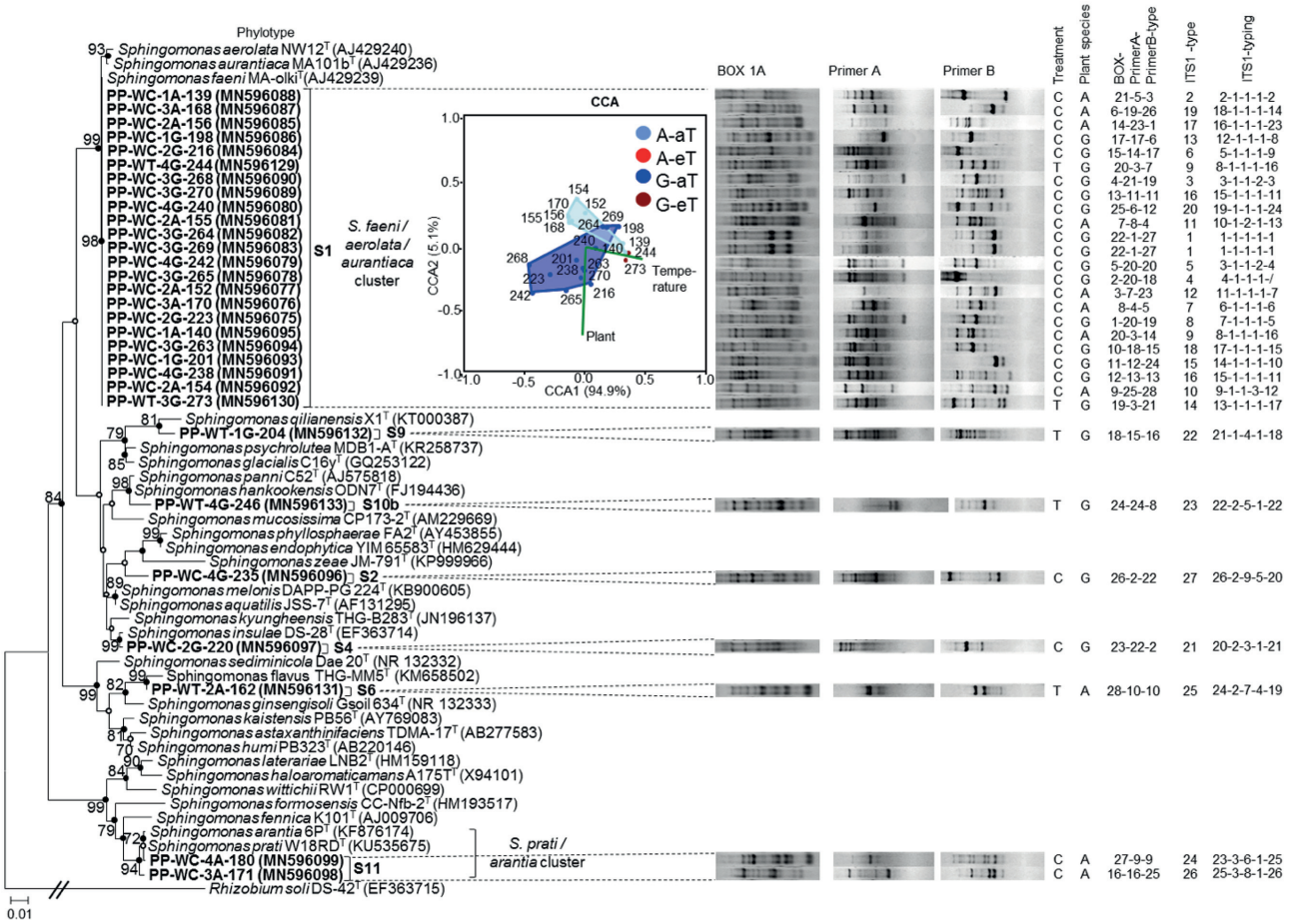

Figure 6. Phylogenetic tree based on nearly full-length 16S rRNA gene sequences showing the phylogenetic relationship of cultured *Sphingomonas* isolates (assigned to different phylotypes: S1, S2, S4, S6, S9, S10b, S11) among each other and to the next related *Sphingomonas* type strains. GenBank accession numbers are given in brackets. The phylogenetic tree was generated with the maximum-likelihood method using Kimura two-parameter model with Gamma distribution and based on 100 replications (bootstrap support) and 1242 nucleotides. Bootstrap values >70% are represented by numbers and branch nodes. Nodes marked with a filled circle were supported with high bootstrap values (>70%), with an unfilled circle were supported with low bootstrap values (<70%) in the neighbor-joining tree. *Rhizobium soli* strain DS-42^T was used as outgroup. Bar: 0.01 substitutions per side. UPGMA cluster analysis of the genomic fingerprint pattern of *Sphingomonas* isolates generated with BOX-PCR and RAPD-PCRs with primers A and B showing the genotypic differences. Clustering considered intensity and presence/absence of DNA bands (Pearson correlation; GelCompar II). Ethidium bromide stained fingerprint patterns separated on an agarose gel (1.5% w/v). M: GeneRuler 100 bp Plus DNA ladder (Thermo Scientific). 16S–23S rRNA gene internal transcribed spacer (ITS-1) sequence analyses of *Sphingomonas* isolates are given and the GenBank accession numbers are listed in Table S1 (Supporting Information). CCA of specific genotypes of the *Sphingomonas* phylotype (S1) and their correlation with environmental factors (temperature, plant species) based on the combined similarity matrix for fingerprint profiles (Box 1A, primer A and primer B) calculated with UPGMA (GelCompar II). Isolates were obtained from *A. elatius* (A) and *G. album* (G) leaves collected from ambient (C) and elevated surface temperature plots (T). 1,2,3,4 = biological replicates (plots). Numbers are standing for the isolate number; each number is representing one bacterial isolate. Analyses were performed in PAST3.

plots independent of the plant species. Isolates of the phylotype M1a shared an intraphylotype similarity of 98.9–100%, of M1b 100% and of M1c 98.9–100%, respectively (Tables S7 and S8b, Supporting Information). Isolates assigned to phylotype M3a were isolated from both plant species grown in T plots (Fig. 5B; Table S7, Supporting Information). The three isolates of phylotype M3a formed a distinct cluster in the phylogenetic tree, closest related to the type strains of *M. mesophilicum*/*M. brachiatum*/*M. pseudosasicola* (Fig. 8). The M3a isolates and the type strain shared 100% sequence similarity among each other (Tables S7 and S8b, Supporting Information).

Methylobacterium isolates were further differentiated by *mxaF* sequencing and genomic fingerprinting. *MxaF* sequences were differentiated at the level of nucleotide (*mxaF* types) and amino acid sequences (MxaF types). A total of six MxaF types were detected representing together 23 *mxaF* types (Fig. 8). Each *Methylobacterium* phylotype represented distinct MxaF types, which indicated functional differences among *Methylobacterium* phylotypes. Isolates of the most isolated phylotype M1a (n = 18) shared the same MxaF type, but showed a high *mxaF*- and genomic fingerprint-type diversity (Fig. 8). Phylotype M1c showed a high genomic-genotype diversity that belonged (except for one isolate) to the same MxaF type, but several *mxaF* types. Phylotype M1b was represented by two isolates, whereby one isolate (grown under heterotrophic growth conditions) originated from *A. elatius* leaves grown in T plots. Those had, next to the different genomic fingerprint type and *mxaF* type, also a different MxaF type, compared to the 100% 16S rRNA gene sequence identical isolate (grown under methylotrophic growth conditions) obtained from *G. album* leaves grown in C plot. The three 16S rRNA gene sequence identical isolates of phylotype M3a represented the same MxaF type, but represented two dif-

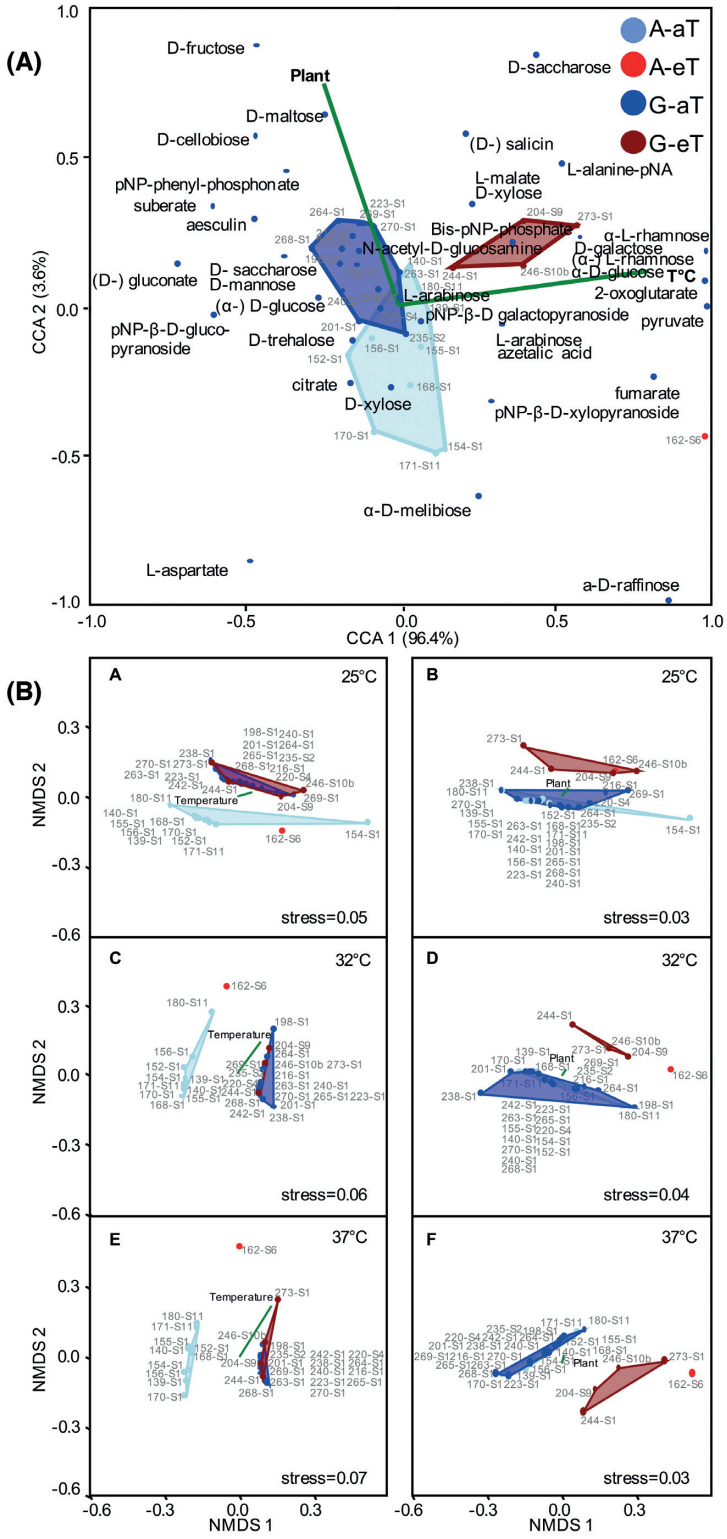

Figure 7. Physiological characterizations of specific *Sphingomonas* isolates. **(A)** CCA of specific *Sphingomonas* phylotypes: S1, S2, S4, S6, S9, S10b, S11 from C and T plots for two plant species, *A. elatius* and *G. album*, including the environmental factors (temperature, plant species) based on the results of carbon substrate utilization and qualitative enzyme test (Kämpfer, Steiof and Dott 1991). The positive/negative matrix of the tests were applied for CCA in the PAST3. aT: ambient surface temperature (control plots); eT: plots with elevated surface temperature +2°C. **(B)** Effect of different temperatures 25°C (a,b), 32°C (c,d) and 37°C (e,f) on average doubling time of the growth. *Sphingomonas* phylotypes: S1, S2, S4, S6, S9, S10b, S11. The average doubling time (in hours) of those phylotypes presented in NMDS using the PAST3 based on a distance matrix calculated with the Bray–Curtis similarity index. The growth of each *Sphingomonas* phylotype was measured in three replicates for each temperature. Scatter plots (a, c, e) present average doubling time and plant species *A. elatius* and *G. album* as environmental factor; scatter plots (b, d, f) present average doubling time and temperature as the second environmental factor. A: *A. elatius*; G: *G. album*. NMDS scatter plots were performed using the PAST3. The significance between C and T plots was determined by one-way ANOSIM test (Bray–Curtis similarity index).

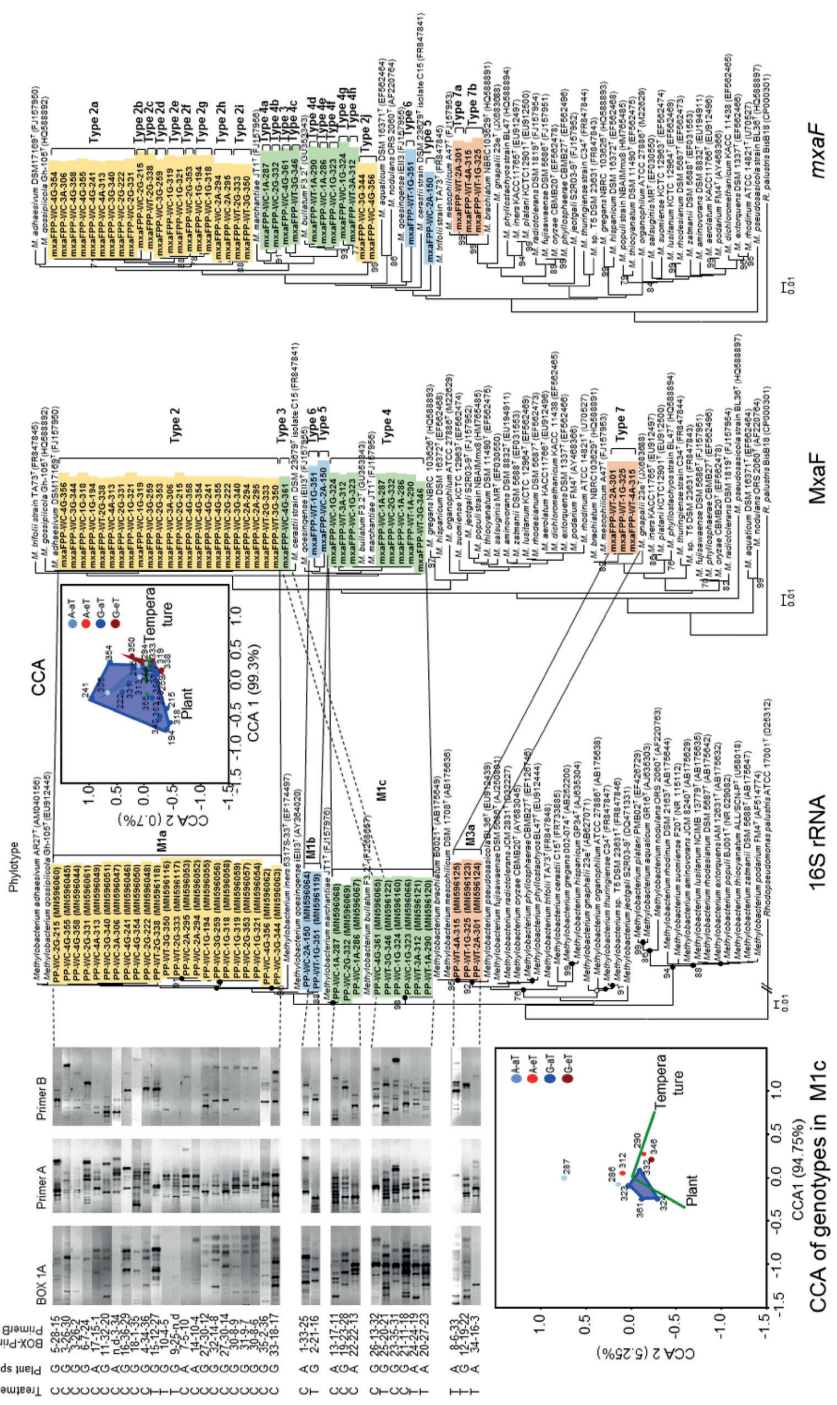

Figure 8. Phylogenetic trees based on nearly full-length 16S rRNA gene sequences and partial *mxaF* nucleotide and amino acid sequences showing the phylogenetic relationships of cultured *Methylobacterium* isolates (assigned to different phylotypes: M1a,b,c, M3a) among each other and to the next related *Methylobacterium* type strains. GenBank accession numbers are given in brackets. The phylogenetic trees based on partial 16S rRNA gene sequences were generated with the maximum-likelihood method using Kimura two-parameter model with Gamma distribution. The phylogenetic trees based on partial *mxaF* nucleotide and amino acid sequence were generated with the neighbor-joining method using Jukes–Cantor correction (*mxaF*) and JTT correction (MxaF). All phylogenetic trees were calculated with 100 replications (bootstrap support) and based on 870 nucleotides (16S rRNA gene sequences), 432 nucleotides (*mxaF* nucleotide sequences) and 141 amino acids (MxaF). Bootstrap values >70% are represented by numbers at branch nodes. Nodes marked with a filled circle were supported with high bootstrap values (>70%), with an unfilled circle were supported with low bootstrap values (<70%) in the neighbor-joining tree. *Rhodopseudomonas palustris* ATCC 17001^{T} and Bis B18 were used as outgroup. Bar: 0.01 substitutions per side. Individual phylotypes (16S rRNA genes based) highlighted in different colors. UPGMA cluster analysis of the genomic fingerprint pattern of *Methylobacterium* isolates generated with BOX-PCR and RAPD-PCRs with primers A and B showing the genotypic differences. Clustering considered intensity and presence/absence of DNA bands (Pearson correlation; GelCompar II). Ethidium bromide stained fingerprint patterns separated on an agarose gel (1.5% w/v). M: GeneRuler 100 bp Plus DNA ladder (Thermo Scientific). CCA depicts the distribution of specific genotypes within the methylotrophic phylotype M1a and M1c separately and their correlation with environmental factors (temperature, plant species) based on the combined similarity matrix for fingerprint profiles (Box 1A, primer A and primer B). Isolates were obtained from *A. elatius* (A) and *G. album* (G) leaves collected from ambient (C) and elevated surface temperature plots (T). 1,2,3,4 = biological replicates (plots). Analyses were performed in PAST3. Individual phylotypes (16S rRNA genes based) highlighted in different colors.

ferent *mxaF* types and three different genomic fingerprint types. CCA analysis showed the highest genetic diversity of M1a isolates cultured from *G. album* plants of C.

DISCUSSION

This study identified specific phylotypes and genotypes of abundant phyllosphere-inhabiting heterotrophic *Sphingomonas* spp. and methylotrophic *Methylobacterium* spp., in response to long-term exposure of elevated surface temperature (+2°C).

Increasing global mean surface temperature affected plants by increasing biomass production (Jansen-Willems *et al.* 2016), and possibly led to enhanced methanol production as by-product of the cell wall synthesis (Sy *et al.* 2005; Abanda-Nkpwatt *et al.* 2006; Kutschera 2007; Schmidt *et al.* 2010). We showed that enhanced surface temperature (+2°C) correlated with an enhanced stomata opening size in leaves of the grass plant. Those changes of the plant physiology and anatomy may have been responsible for the changes in composition and diversity of the studied leaf microbiota.

Warming effects on plant physiology and anatomy

This and other research of the same study (Jansen-Willems *et al.* 2016) showed that increased surface warming affected plants directly, i.e. aboveground plant biomass yield was higher in T compared to C plots, in line with other studies (Luo 2007; Ma *et al.* 2010). The response of plant growth to climate change is growth season specific; previous studies reported a positive effect of warming on the aboveground biomass in spring and a negative effect in summer (Luo 2007; Luo, Sherry and Zhou 2009; Ma *et al.* 2010). More water uptake from the soil is needed with increasing biomass, which, depending on the duration and frequency, leads to water stress and affects the microbiome via different stomata openings (Porporato, Daly and Rodriguez-Iturbe 2004; Knapp *et al.* 2008). Other studies showed an interaction such as precipitation and warming (Ma *et al.* 2010; Lin *et al.* 2016). Plants enhance their stomata opening for an efficient cooling by transpiration (Feller 2006) as a reaction of warming, but only one report considered the effects on stomata (aperture) size (Zheng *et al.* 2013) as shown in our study on *A. elatius* from T plots. Zheng *et al.* (2013) observed a reduction of stomata aperture size for maize with warming indicating a dependency on plant species and the water availability.

Another important finding of the current study was the change in leaf metabolites with warming for both plant species. Gargallo-Garriga *et al.* (2017) showed that warming on a grass and a herb from an Iceland grassland caused a change in the metabolome under long-term warming (>50 years).

Especially, metabolic pathways, including most of the saccharides, amino acids and the secondary metabolites as phenolic acids and terpenes, were upregulated, and involved in the plant stress response (Gargallo-Garriga *et al.* 2017). The plant physiology and anatomy led to changes in the nutritional and environmental base for phyllosphere-inhabiting bacteria.

Warming effects on the total cell numbers and the importance of the leaf structure

The plant leaf structure plays also an important role for the colonization of the phyllosphere. The concentration of total leaf-associated cells was higher for *A. elatius*, while the concentration of culturable bacteria was always higher on *G. album* leaves. A reason could be that phyllosphere bacteria on leaves of the grass plant (*A. elatius*) could be easily washed away by precipitation due to leaf position in comparison to the dicotyledonous plant *G. album*. Regarding the current experiment, 1 h before sampling a finer rain/drizzle (precipitation 0.1 mm) began and continued during the sampling for ∼2 h. Moreover, two days before sampling it rained also for several hours.

Both leaf sides of the grass plant were affected by these weather conditions in contrast to the dicotyledonous plant, whose bottom leaf side was protected. In addition, more loosely attached bacteria that can easily be washed away were associated with *A. elatius*. However, more bacterial aggregates may have been washed away from *G. album* leaves, which might explain the higher concentrations of culturable bacteria on this dicot species. Moreover, higher bacterial population was detected closer to the soil surface as revealed by Kinkel, Wilson and Lindow (2000) and Wellner, Lodders and Kämpfer (2011). Thus, *G. album* leaves presented a more protected physical environment to phyllospheric bacteria compared to leaves of *A. elatius* especially after rainfall events. Also, the difference in plant size affected the distance of the leaves to the IR heaters possibly resulting in different leaf surface temperatures of *G. album* and *A. elatius*.

Warming effects on the total leaf-associated microbial community and concentration and community composition of culturable heterotrophs and methylotrophs

Elevated surface temperature had led to significantly lower concentrations of total heterotrophs and methylotrophs as well as PPFMs under methylotrophic growth conditions only on leaves of *G. album*. Wellner, Lodders and Kämpfer (2011) reported that *Methylobacterium* spp. numbers were mainly influenced by the combination of environmental factors such as plant species, sampling site and observation period possibly explaining the different effects of elevated temperature on the concentrations of culturable heterotrophs and methylotrophs.

Elevated surface temperature led to a shift in the microbiome composition for both plants. Our results indicated an increase in the variability and diversity of the most abundant cultured heterotrophs and methylotrophs in T plots. This was congruent with the data of the culture-independent approach, which showed an increased bacterial diversity with elevated temperature (Aydogan *et al.* 2018) revealing different abundant heterotrophic bacteria for both plants under elevated surface temperature (Fig. 5A) and in line with results from similar studies on grassland (Sheik *et al.* 2011) and other plants (Rastogi *et al.* 2012).

Warming effect on abundant culturable phyllosphere inhabitants

At the genus level, *Sphingomonas* and *Methlyobacterium* were the most abundant culturable heterotrophic and methylotrophic bacteria of both plant species, as also observed by others (Delmotte *et al.* 2009; Innerebner, Knief and Vorholt 2011; Knief *et al.* 2012; Bodenhausen, Horton and Bergelson 2013). However, the results of Saleem *et al.* (2017) and Pineda *et al.* (2013) could not be confirmed, who indicated a recruitment of beneficial microbes by plants under stressed conditions.

Under heterotrophic growth conditions, *Sphingomonas* phylotypes were frequently detected on both plant species with very

low frequency from plots treated with elevated surface temperature. This was confirmed by the cultivation-independent studies. The importance and function of *Sphingomonas* in the phyllosphere were previously discussed in detail (Aydogan *et al.* 2018). Here, we revealed that changes of *Sphingomonas* abundance correlated with changes in the metabolite profile of leaves (see the discussion below).

A reduced abundance at elevated surface temperature was also obtained for *Methylobacterium* spp. cultured under heterotrophic growth conditions. Cultivation-independent studies confirmed the lower abundance of *Methylobacterium* spp. on leaves of both plant species from T plots. Regarding the plant beneficial effects of *Methylobacterium* spp. (Abanda-Nkpwatt *et al.* 2006; Lee *et al.* 2006; Ryu *et al.* 2006), a negative effect of elevated surface temperature on this genus would accompany a negative effect on plant growth and health.

The majority of the identified *Methylobacterium* spp. (27/31 isolates) isolated from methylotrophic growth conditions were assigned to phylotypes M1a and M1c that were found in all replicates independent of the temperature treatment. This indicates that elevated surface temperature directly or indirectly did not affect the growth of these abundant *Methlyobacterium* phylotypes on leaves of both plant species. One reason could be that *Methylobacterium* spp. profit from being specialists and are related to one-carbon metabolism and hence do not need to compete for other carbon compounds (e.g. sugars) like the big variety of heterotrophic bacteria (Sy *et al.* 2005), which occur at higher concentrations (CFU g^{-1}) than methylotrophs.

Thus, warming effects on *Methylobacterium* spp. occurrence depend on their nutritional preference.

Warming effects on specific phylo- and genotypes of *Sphingomonas* and *Methylobacterium* isolates

Specific *Sphingomonas* and *Methylobacterium* phylotypes only occurred under elevated temperature conditions and/or only in the phyllosphere of *G. album* or *A. elatius*. This indicated a functional adaptation of these phylotypes to higher temperatures. Van der Walt *et al.* (2016) mentioned unique habitat-specific phylotypes by analyzing the soil microbiota of fairy circles surrounded by grass species. Ecotypes can appear to persist in complex communities at an extremely fast rate (Doolittle and Zhaxybayeva 2009), indicating a fast adaptation to climate change. The differentiation of abundant cultivated *Sphingomonas* and *Methylobacterium* isolates at the genotypic level indicated a genetic adaptation to enhanced surface temperature on species and intraspecies levels that are not plant species specific (Figs 6–8). Ellis, Thompson and Bailey (1999) also found that specific *Pseudomonas* genotypes were able to adapt to defined environmental conditions surviving at low population densities under changing environmental conditions. Cohan (2002) described the adaptation of specific 'ecotypes' of one species to changed conditions, which were confirmed by Koeppel *et al.* (2008) by analyzing two *Bacillus* clades from the 'Evolution Canyons' of Israel. Here, we showed that some phylotypes of the genera *Sphingomonas* and *Methlyobacterium* were only found under elevated surface temperature, which demonstrated an ecological adaptation of these organisms to warming.

CONCLUSION

The study provided a clear indication that increasing surface temperature leads to changes in the leaf anatomy and plant physiology of different plant species affecting the concentration and composition of total as well as culturable heterotrophic and methylotrophic bacteria in their phyllosphere. The occurrence of specific bacterial phylotypes in the phyllosphere under enhanced surface temperature, especially *Sphingomonas* and *Methlyobacterium* phylotypes, revealed an ecotype adaptation to elevated surface temperature in a permanent grassland.

We provide evidence of a decrease in the amount of heterotrophic *Sphingomonas* under elevated temperature. This finding raises the question whether changes in the leaf metabolites or changes in surface temperature were the predominant factors leading to those changes. The studies on *Sphingomonas* isolates provided a strong hint that both factors were involved to explain the changes. *Sphingomonas* isolated from leaves of plants grown under increased surface temperature were physiologically adapted with respect to temperature-dependent growth maxima and to changes in the substrate utilization patterns. However, more detailed studies are needed to confirm the findings. The role of *Sphingomonas* as key taxa was already discussed in previous studies (Aydogan *et al.* 2018). Here, we showed that the decreased abundance of *Sphingomonas* correlated with an increased bacterial diversity. Several bacteria, which may be better adapted to increased temperature or changing water potential in the phyllosphere, as *Nocardioides* species (Yoon and Park 2006) occurred under elevated temperature, but also plant pathogens increased in relative abundance. Further field studies and studies on model organisms under controlled laboratory conditions and considering several sampling time points would be helpful to identify whether this effect is ubiquitous and how this may affect plant health.

SUPPLEMENTARY DATA

Supplementary data are available at *FEMSEC* online.

AUTHORS AND CONTRIBUTORS

ELA, OB and SPG analyzed the data and wrote the manuscript; ABJ-W, GM and CM planned and performed the field experiment; SPG and ELA planned the phyllosphere study; SPG, ELA and GM performed the phyllosphere sampling; ELA and MH performed SEM analysis; YHC performed the metabolome analysis; ELA prepared respective samples; and OB performed experimental and statistical analysis of physiological and temperature-dependent growth experiments of *Sphingomonas* isolates. ELA and PK received the funding, and all authors improved the final manuscript version.

ACKNOWLEDGMENTS

We thank Lisa Anweiler for her help in the cultivation of bacterial isolates.

FUNDING

This work is part of the LOEWE research initiative network FACE2FACE, which is funded by the Hessian Ministry for Science and Arts. We acknowledge the long-term funding of the Environmental Monitoring and Climate Change Impact Research Station Linden by the Hessian Agency for Nature Conservation, Environment and Geology (HLNUG).

Conflict of interest. There are no relevant conflicts of interest.

REFERENCES

Abanda-Nkpwatt D, Müsch M, Tschiersch J *et al*. Molecular interaction between *Methylobacterium extorquens* and seedlings: growth promotion, methanol consumption, and localization of the methanol emission site. *J Exp Bot* 2006;**57**:4025–32.

Arenz BE, Schlatter DC, Bradeen JM *et al*. Blocking primers reduce co-amplification of plant DNA when studying bacterial endophyte communities. *J Microbiol Methods* 2015;**117**:1–3.

Aydogan EL, Busse HJ, Moser G *et al*. *Aureimonas galii* sp. nov. and *Aureimonas pseudogalii* sp. nov. isolated from the phyllosphere of *Galium album*. *Int J Syst Evol Microbiol* 2016;**6**:3345–54.

Aydogan EL, Moser G, Müller C *et al*. Long-term warming shifts the composition of bacterial communities in the phyllosphere of *Galium album* in a permanent grassland field-experiment. *Front Microbiol* 2018;**9**:144.

Bodenhausen N, Horton MW, Bergelson J. Bacterial communities associated with the leaves and the roots of *Arabidopsis thaliana*. *PLoS One* 2013;**8**:e56329.

Bringel F, Couée I. Pivotal roles of phyllosphere microorganisms at the interface between plant functioning and atmospheric trace gas dynamics. *Front Microbiol* 2015;**6**:486.

Cohan FM. What are bacterial species? *Ann Rev Microbiol* 2002;**56**:457–87.

Delmotte N, Knief C, Chaffron S *et al*. Community proteogenomics reveals insights into the physiology of phyllosphere bacteria. *Proc Natl Acad Sci USA* 2009;**106**:16428–33.

Doolittle WF, Zhaxybayeva O. On the origin of prokaryotic species. *Genome Res* 2009;**19**:744–56.

Ellis RJ, Thompson IP, Bailey MJ. Temporal fluctuations in the pseudomonad population associated with sugar beet leaves. *FEMS Microbiol Ecol* 1999;**28**:345–56.

Feller U. Stomatal opening at elevated temperature: an underestimated regulatory mechanism. *Gen Appl Plant Physiol* 2006;**3**:19–31.

Fisher M, Triplett EW. Automated approach for ribosomal intergenic spacer analysis of microbial diversity and its application to freshwater bacterial communities. *Appl Environ Microb* 1999;**65**:4630–6.

Gargallo-Garriga A, Ayala-Roque M, Sardans J *et al*. Impact of soil warming on the plant metabolome of Icelandic grasslands. *Metabolites* 2017;**7**:44.

Glaeser SP, Galatis H, Martin K *et al*. *Niabella hirudinis* and *Niabella drilacis* sp. nov., isolated from the medicinal leech *Hirudo verbana*. *Int J Syst Evol Microbiol* 2013;**63**:3487–93.

Glenn DM, Bassett C, Dowd SE. Effect of pest management system on 'Empire' apple leaf phyllosphere populations. *Sci Hortic* 2015;**183**:58–65.

Hammer Ø, Harper DAT, Ryan PD. PAST: paleontological statistics software package for education and data analysis. *Palaeontol Electron* 2001;**4**:1–9.

Innerebner G, Knief C, Vorholt JA. Protection of *Arabidopsis thaliana* against leaf-pathogenic *Pseudomonas syringae* by *Sphingomonas* strains in a controlled model system. *Appl Environ Microb* 2011;**77**:3202–10.

IPCC. Climate Change 2013: The Physical Science Basis. In: Stocker TF, Qin D, Plattner G-K et al. (eds.). *Contribution of Working Group I to the Fifth Assessment Report of the Intergovernmental Panel on Climate Change*. Cambridge, United Kingdom and New York, NY, USA: Cambridge University Press, 2013, 1535.

Jansen-Willems AB, Lanigan GJ, Grünhage L *et al*. Carbon cycling in temperate grassland under elevated temperature. *Ecol Evol* 2016;**6**:7856–68.

Jones DT, Taylor WR, Thornton JM. The rapid generation of mutation data matrices from protein sequences. *Bioinformatics* 1992;**8**:275–82.

Jo Y, Cho JK, Choi H *et al*. Bacterial communities in the phylloplane of *Prunus* species. *J Basic Microb* 2015;**55**:504–8.

Jukes TH, Cantor CR. Evolution of protein molecules. In: Munro HN (ed) . *Mammalian Protein Metabolism*. New York: Academic Press, 1969, 21–132.

Kim HK, Choi YH, Verpoorte R. NMR-based metabolomic analysis of plants. *Nat Protoc* 2010;**3**;536–49.

Kinkel LL, Wilson M, Lindow SE. Plant species and plant incubation conditions influence variability in epiphytic bacterial population size. *Microbial Ecol* 2000;**39**:1–11.

Knapp AK, Beier C, Briske DD *et al*. Consequences of more extreme precipitation regimes for terrestrial ecosystems. *AIBS Bull* 2008;**58**:811–21.

Knief C, Delmotte N, Chaffron S *et al*. Metaproteogenomic analysis of microbial communities in the phyllosphere and rhizosphere of rice. *ISME J* 2012;**6**:1378–90.

Koeppel A, Perry EB, Sikorski J *et al*. Identifying the fundamental units of bacterial diversity: a paradigm shift to incorporate ecology into bacterial systematics. *Proc Natl Acad Sci USA* 2008;**105**:2504–9.

Kutschera U. Plant-associated methylobacteria as co-evolved phytosymbionts: a hypothesis. *Plant Signal Behav* 2007;**2**:74–8.

Kämpfer P, Steiof M, Dott W. Microbiological characterisation of a fuel-oil contaminated site including numerical identification of heterotrophic water and soil bacteria. *Microb Ecol* 1991;**21**:227–51.

Lee HS, Madhaiyan M, Kim CW *et al*. Physiological enhancement of early growth of rice seedlings (*Oryza sativa* L.) by production of phytohormone of N_2-fixing methylotrophic isolates. *Biol Fert Soils* 2006;**42**:402–8.

Leveau JHJ, Tech JJ. Grapevine microbiomics: bacterial diversity on grape leaves and berries revealed by high-throughput sequence analysis of 16S rRNA amplicons. *Acta Hortic* 2011;**905**:31–42.

Lindow SE, Brandl MT. Microbiology of the phyllosphere. *Appl Environ Microb* 2003;**69**:1875–83.

Lin L, Zhu B, Chen C *et al*. Precipitation overrides warming in mediating soil nitrogen pools in an alpine grassland ecosystem on the Tibetan Plateau. *Sci Rep* 2016;**6**:31438.

Ludwig W, Strunk O, Westram R *et al*. ARB: a software environment for sequence data. *Nucleic Acids Res* 2004;**32**:1363–71.

Lunau M, Lemke A, Walther K *et al*. An improved method for counting bacteria from sediments and turbid environments by epifluorescence microscopy. *Environ Microbiol* 2005;**7**:961–8.

Luo Y, Sherry R, Zhou X *et al*. Terrestrial carbon-cycle feedback to climate warming: experimental evidence on plant regulation and impacts of biofuel feedstock harvest. *GCB Bioenergy* 2009;**1**:62–74.

Luo Y. Terrestrial carbon-cycle feedback to climate warming. *Annu Rev Ecol Evol S* 2007;**1**:683–712.

Ma W, Liu Z, Wang Z *et al*. Climate change alters interannual variation of grassland aboveground productivity: evidence from a 22-year measurement series in the Inner Mongolian grassland. *J Plant Res* 2010;**123**:509–17.

McDonald IR, Kenna EM, Murrell JC. Detection of methanotrophic bacteria in environmental samples with the PCR. *Appl Environ Microb* 1995;**61**:116–21.

Muyzer G, De Waal EC, Uitterlinden AG. Profiling of complex microbial populations by denaturing gradient gel electrophoresis analysis of polymerase chain reaction-amplified genes coding for 16S rRNA. *Appl Environ Microb* 1993;**59**:659–700.

Pineda A, Dicke M, Pieterse CM *et al.* Beneficial microbes in a changing environment: are they always helping plants to deal with insects?. *Funct Ecol* 2013;**27**:574–86.

Porporato A, Daly E, Rodriguez-Iturbe I. Soil water balance and ecosystem response to climate change. *Am Nat* 2004;**164**:625–32.

Rastogi G, Sbodio A, Tech JJ *et al.* Leaf microbiota in an agroecosystem: spatiotemporal variation in bacterial community composition on field-grown lettuce. *ISME J* 2012;**6**:1812–22.

Ren G, Zhang H, Lin X *et al.* Response of phyllosphere bacterial communities to elevated CO_2 during rice growing season. *Appl Microbiol Biot* 2014;**98**:9459–71.

Ren G, Zhu C, Alam MS *et al.* Response of soil, leaf endosphere and phyllosphere bacterial communities to elevated CO_2 and soil temperature in a rice paddy. *Plant Soil* 2015;**392**:27–44.

Rico L, Ogaya R, Terradas J *et al.* Community structures of N_2-fixing bacteria associated with the phyllosphere of a Holm oak forest and their response to drought. *Plant Biol* 2014;**16**:586–93.

Rodwell JS, Pigott CD, Ratcliffe DA *et al. British Plant Communities. Grasslands and Montane Communities*. Vol. **3**. Cambridge: Cambridge University Press, 1992.

Ryu J, Madhaiyan M, Poonguzhali S *et al.* Plant growth substances produced by *Methylobacterium* spp. and their effect on tomato (*Lycopersicon esculentum* L.) and red pepper (*Capsicum annuum* L.) growth. *J Microbiol Biotechnol* 2006;**16**:1622–8.

Saleem M, Meckes N, Pervaiz ZH *et al.* Microbial interactions in the phyllosphere increase plant performance under herbivore biotic stress. *Front Microbiol* 2017;**8**:41.

Schmidt S, Christen P, Kiefer P *et al.* Functional investigation of methanol dehydrogenase-like protein XoxF in *Methylobacterium extorquens* AM1. *Microbiology* 2010;**156**:2575–86.

Sheik CS, Beasley WH, Elshahed MS *et al.* Effect of warming and drought on grassland microbial communities. *ISME J* 2011;**5**:1692–700.

Sy A, Timmers AC, Knief C *et al.* Methylotrophic metabolism is advantageous for *Methylobacterium extorquens* during colonization of *Medicago truncatula* under competitive conditions. *Appl Environ Microb* 2005;**71**:7245–52.

Tamura K, Peterson D, Peterson N *et al.* MEGA5: Molecular Evolutionary Genetics Analysis using maximum likelihood, evolutionary distance, and maximum parsimony methods. *Mol Biol Evol* 2011;**28**:2731–9.

Thompson JD, Higgins DG, Gibson TJ. CLUSTAL W: improving the sensitivity of progressive multiple sequence alignment through sequence weighting, position-specific gap penalties and weight matrix choice. *Nucleic Acids Res* 1994;**22**:4673–80.

Trouvelot S, Héloir MC, Poinssot B *et al.* Carbohydrates in plant immunity and plant protection: roles and potential application as foliar sprays. *Front Plant Sci* 2014;**5**:592.

Van der Walt AJ, Johnson RM, Cowan DA *et al.* Unique microbial phylotypes in Namib Desert dune and gravel plain fairy circle soils. *Appl Environ Microb* 2016;**82**:4592–601.

Versalovic J, Schneider M, de Bruijn FJ *et al.* Genomic fingerprinting of bacteria using repetitive sequence-based polymerase chain reaction. *Method Mol Cell Biol* 1994;**5**:25–40.

Vorholt JA. Microbial life in the phyllosphere. *Nat Rev Microbiol* 2012;**10**:828–40.

Wellner S, Lodders N, Glaeser SP *et al. Methylobacterium trifolii* sp. nov. and *Methylobacterium thuringiense* sp. nov., methanol-utilizing, pink-pigmented bacteria isolated from leaf surfaces. *Int J Syst Evol Microbiol* 2013;**63**:2690–9.

Wellner S, Lodders N, Kämpfer P. Diversity and biogeography of selected phyllosphere bacteria with special emphasis on *Methylobacterium* spp. *Syst Appl Microbiol* 2011;**34**:621–30.

Yarza P, Richter M, Peplies J *et al.* The All-Species Living Tree project: a 16S rRNA-based phylogenetic tree of all sequenced type strains. *Syst Appl Microbiol* 2008,**31**:241–50.

Yashiro E, McManus PS. Effect of streptomycin treatment on bacterial community structure in the apple phyllosphere. *PLoS One* 2012;**7**:e37131.

Yoon J-H, Park Y-H. The genus *Nocardioides*. *Prokaryotes* 2006;**3**:1099–113.

Yoon SH, Ha SM, Kwon S *et al.* Introducing EzBioCloud: a taxonomically united database of 16S rRNA and whole genome assemblies. *Int J Syst Evol Micr* 2017;**67**:1613–17.

Zheng Y, Xu M, Hou R *et al.* Effects of experimental warming on stomatal traits in leaves of maize (*Zea may* L.). *Ecol Evol* 2013;**3**:3095–111.

Ziemke F, Brettar I, Höfle MG. Stability and diversity of the genetic structure of a *Shewanella putrefaciens* population in the water column of the central Baltic. *Aquat Microb Ecol* 1997;**13**:63–74.